Synthesis and characterization of novel chitosan-dopamine or chitosan-tyrosine conjugates for potential nose-to-brain delivery

Roberta Cassano[a], Adriana Trapani[b,*], Maria Luisa Di Gioia[a], Delia Mandracchia[a,1], Rosalia Pellitteri[c], Giuseppe Tripodo[d], Sonia Trombino[a], Sante Di Gioia[e,*], Massimo Conese[e]

[a] Department of Pharmacy, Health and Nutritional Sciences, University of Calabria, 87036 Arcavacata di Rende, Cosenza, Italy
[b] Department of Pharmacy-Drug Sciences, University of Bari "Aldo Moro", 70125 Bari, Italy
[c] Institute for Biomedical Research and Innovation (IRIB-CNR), 95126 Catania, Italy
[d] Department of Drug Sciences, University of Pavia, 27100 Pavia, Italy
[e] Department of Medical and Surgical Sciences, University of Foggia, 71122 Foggia, Italy

ARTICLE INFO

This work is dedicated to the memory of Prof. Nevio Picci

Keywords:
Chitosan derivatives
Dopamine
Mucoadhesion
Uptake
Nose-to-brain delivery

ABSTRACT

This work aims to the synthesis of novel carboxylated chitosan-dopamine (DA) and -tyrosine (Tyr) conjugates as systems for improving the brain delivery of the neurotransmitter DA following nasal administration. For this purpose, ester or amide conjugates were synthesized by *N*,*N*-dicyclohexylcarbodiimide (DCC) mediated coupling reactions between the appropriate *N*-*tert*-butyloxycarbonyl (Boc) protected starting polymers *N*,*O*-carboxymethyl chitosan and 6-carboxy chitosan and DA or *O*-*tert*-Butyl-L-tyrosine-*tert*-butyl ester hydrochloride. The resulting conjugates were characterized by FT-IR and ^{1}H- and ^{13}C NMR spectroscopies and their *in vitro* mucoadhesive properties in simulated nasal fluid (SNF), toxicity and uptake from Olfactory Ensheathing Cells (OECs) were assessed. Results demonstrated that *N*,*O*-carboxymethyl chitosan-DA conjugate was the most mucoadhesive polymer in the series examined and, together with the 6-carboxy chitosan-DA-conjugate were able to release the neurotransmitter in SNF. The MTT assay showed that the starting polymers as well as all the prepared conjugates in OECs resulted not toxic at any concentration tested. Likewise, the three synthesized conjugates were not cytotoxic as well. Cytofluorimetric analysis revealed that the *N*,*O*-carboxymethyl chitosan DA conjugate was internalized by OECs in a superior manner at 24 h as compared with the starting polymer. Overall,the *N*,*O*-CMCS-DA conjugate seems promising for improving the delivery of DA by nose-to-brain administration.

1. Introduction

Parkinson's disease (PD) is a progressive neurodegenerative dis- order whose main hallmarks are represented by loss of dopaminergic neurons in the Substantia Nigra *pars compacta* and the presence of Lewy bodies abnormal protein aggregates including α-synuclein and ubi- quitin (Di Stefano et al., 2009; Di Gioia et al., 2015; Rodriguez-Nogaleset al., 2016). As a consequence of the decrease in dopaminergic neu-rons, particularly at level of the striatum brain region, several motor and non-motor symptoms are present in the course of the disease, such as tremor, bradykinesia and sleep disorders, respectively (Rodriguez-Nogales et al., 2016). Although the pathogenesis of PD is still unknown, it seems to be accepted that aging is the main risk factor leading to a loss of compensatory mechanisms of the neurological damage processes (Rodriguez-Nogales et al., 2016). To date, the standard treatment for controlling PD motor symptoms is based on the so called dopamine (DA) replacement strategy which aims to compensate for the loss of dopaminergic neurons and re-establish satisfactory levels of the neurotransmitter. In this context, Levodopa (L-Dopa), which may be considered a biological precursor of DA, still constitutes the most effective and reference drug (Di Stefano et al., 2009; Rodriguez-Nogales et al., 2016). DA is unable to overcome the blood-brain-barrier (BBB) because of its high hydrogen bonding potential, complete ionization at physio- logical pH, and extensive metabolism by the oral route of administra- tion (Di Gioia et al., 2015). In contrast, L-Dopa can cross the BBB ex- ploiting an active transport system and is converted to DA by fast enzymatic decarboxylation due to L-Dopa-decarboxylase in the brain (Di Gioia et al., 2015; Trapani et al., 2017). As occurs for many other neurodegenerative diseases, even for the PD treatment, the main goal is the BBB overcoming by the biologically active substance, along with its

* Corresponding authors.
E-mail addresses: adriana.trapani@uniba.it (A. Trapani), sante.digioia@unifg.it (S. Di Gioia).
[1] Present address: Department of Molecular and Translational Medicine, University of Brescia, Viale Europa 11, Brescia, 25123, Italy.

sustained release in appropriate brain regions and reduction of its inherent toxic effects (Rodriguez-Nogales et al., 2016). In this regard, the promising role played by nanostructured drug delivery systems has been pointed-out (Re et al., 2012; Hawthorne et al., 2016; Rodriguez- Nogales et al., 2016). Several parameters influence the efficiency of BBB penetration by nanocarriers including their size, shape and zeta potential (Saraiva et al., 2016). It seems that a common characteristic of such kind of nanocarriers is their ability to interact with the BBB, ex- ploiting the existing transport mechanisms such as receptor- and ad- sorptive-mediated transcytosis or their ability to open the tight junc- tions between the BBB cells. It can be obtained by an appropriate surface modification of the nanovehicle, including coating with sur- factant (*e.g.*, polysorbate 80 or polyethylene glycol etc.) or using a nanosystem endowed with a positive surface charge to allow electro-
static interactions with the negatively charged BBB or employing a nanomaterial capable of opening the tight junctions of epithelial cells(*e.g.*, chitosan) (Re et al., 2012; Hawthorne et al., 2016; Rodriguez- Nogales et al., 2016). Thus, most interest has been focused on the de- velopment of DA-loaded nanocarriers as innovative PD treatment, since they may be able to cross the BBB enabling also a sustained delivery of the neurotransmitter to the brain (Pillay et al., 2009; De Giglio et al., 2011; Trapani et al., 2011; Re et al., 2012; Pahuja et al., 2015; Rashedet al., 2015; Hawthorne et al., 2016; Rodriguez-Nogales et al., 2016). However, in these DA-loaded polymer based nanocarriers, the neuro-transmitter is entrapped in the polymeric matrix and its leakage from the delivery system could occur. Alternatively, an interesting option is to link DA to a polymeric backbone by a cleavable bond leading to a polymeric DA conjugate which may be administered as such or as a nanostructured carrier. Using these conjugates, it is possible to over-come the BBB as well as to obtain a targeted and sustained release of the
neurotransmitter at site of action and reduced toxic effects (Re et al., 2012; Saraiva et al., 2016).

In alternative to cross the BBB, a valuable and most investigated possibility is represented by the delivery of therapeutic agents to the brain using nanosystems by nasal route (Mistry et al., 2009, 2015; Mdet al., 2014). In this regard, the role of nanocarriers in nose-to-brain drug delivery has been recently discussed and it has been evidencedthat extending nasal residence time and maintenance of high local drug concentration improves this delivery method (Feng et al., 2018). Moreover, some nanovehicle features including particle size, surface charge, surface modification and nasal mucociliary clearance influen- cing nose-to-brain delivery have been identified and analyzed (Feng et al., 2018).

In literature, some polymer-DA conjugates are described comprising both natural and synthetic polymers. Thus, among the natural polymer-DA conjugates, the hyaluronic acid-DA (Kim et al., 2014; Neto et al., 2014), starch-DA (Shi et al., 2018) and gelatin-DA (Fan et al., 2016) conjugates have been reported, while poly[α,β-(*N*-2-hydroxyethyl-DL-aspartamide)]-DA styrene-maleic anhydride copolymer-DA and poly-DL-(2,5-dioxo-l,3-pyrrolidinediyl)-DA as well as poly(aspartamide)-DA conjugates have been described as examples of synthetic polymer-DA conjugates (Kalčić et al., 1996; Juriga et al., 2018). In these conjugates, DA is linked to the polymeric chain through an amide bond exploiting the amine functional group of the neurotransmitter.

The aim of this work was the synthesis, characterization and assessment of *in vitro* toxicity and internalization of novel CS-DA conjugates [*i.e.*, *N*,*O*-carboxymethyl chitosan (*N*,*O*-CMCS)-DA and *N*,*O*-CMCS-Tyrosine (Tyr) conjugates **1c** and **1e**, respectively, as well as 6-carboxy chitosan (6-CarboxyCS)-DA conjugate **2c** (Scheme 1)] for potential nose-to-brain DA delivery. Our interest was not only for the neurotransmitter DA as such but also for the amino acid Tyr which, once released from the corresponding conjugate, is expected to be converted *in vivo* in L-DOPA (the endogenous precursor of DA) thanks to the enzyme tyrosine hydroxylase, although the enzyme levels are low in advanced Parkinson's disease (Kordower et al., 2013; Nagatsu et al., 2019). In details, conjugates **1c** and **2c** the neurotransmitter is linked to the chitosan (CS) derivative through an ester bond exploiting the ca-techol group, whereas in conjugate **1e** Tyr is connected to *N*,*O*-CMCS*via* an amide bond. To the best of our knowledge, polymer-DA con- jugates, characterized by an ester bond linkage, have not been pre- viously described in literature. CS is a well-known mucoadhesive polymer mostly used for drug delivery and tissue engineering purposes because of its biocompatibility, biodegradability and absorption en- hancement (Dash et al., 2011). Several chemical modifications have been performed to improve not only the mucoadhesive properties of CS (Bonengel and Bernkop-Schnurch, 2014; Trapani et al., 2014), but also the solubility performance in neutral and alkaline media of this polymer. Glycol CS and *N*,*O*-CMCS are well known CS derivatives en-dowed with better aqueous solubility at neutral and physiological conditions (Anitha et al., 2009; Mandracchia et al., 2017a). Herein, we
describe the synthesis of conjugates **1c**, **1e** and **2c** (Scheme 1), and the evaluation of their mucoadhesive properties and DA release kinetics. Moreover, to gain insights into their potential for nose-to-brain administration, the cytotoxicity and uptake by Olfactory Ensheathing Cells (OECs), a special type of glial cells, were also determined.

2. Materials and methods

2.1. Materials

N,*O*-Carboxymethyl Chitosan **1** (*N*,*O*-CMCS, Molecular weight in the range of 30–500 kDa, deacetylation degree, 94.2%; viscosity22 mPa·sec, Fig. 1) was purchased from Heppe Medical Chitosan GmbH (Halle, Germany). Chitosan (CS, medium molecular weight, deacetylation degree 75–85%, viscosity 200–800 mPa·sec), dicyclohexylcarbodiimide (DCC), di-*tert*-butyl dicarbonate (Boc_2O), 4-dimethylaminopyridine (DMAP), anhydrous *N*,*N*-dimethylformamide (DMF), trifluoroacetic acid (TFA), dichloromethane (DCM), dimethylsulfoxide (DMSO), dopamine hydrochloride (DA), porcine stomach mucin (type II, bound sialic acid ~1%), Fluorescein 5(6)-isothiocyanate (FITC), sodium nitrite ($NaNO_2$), formic acid 85%, methylene blue, sodium bicarbonate, citric acid, sodium sulfate, 1-butyl-3-methyl imidazolium tetrafluoroborate [Bmim] [BF_4], cytosine arabinoside, Dulbecco's Modified Eagle's medium (DMEM), Foetal Bovine Serum (FBS) and PBS were purchased from Sigma-Aldrich (Milan, Italy). *O*-*tert*-Butyl-L-tyrosine-*tert*-butyl ester hydrochloride [H-Tyr(OtBu)-OtBu·HCl] was purchased from Bachem AG (Bubendorf, Switzerland). Hydroxyethyl cellulose (HEC, Natrosol 250) was provided by Aakon Polichimica (Milan, Italy). According to manufacturer instructions, the viscosity of a solu- tion of HEC at the concentration of 2% in water was equal to 5500 mPa·sec. Dialysis tubes with a MWCO 12–14 kDa were purchased from Spectra Labs. Throughout this work, double distilled water wasused. All other chemicals used were of reagent grade.

2.2. Apparatus

The prepared conjugates were characterized by FT-IR, ^{1}H- and, in some cases, ^{13}C NMR spectroscopy. Proton nuclear magnetic resonance (^{1}H NMR) spectra were recorded on a Brüker spectrometer at 300 MHz. The analyses were performed at 293 °K on dilute solutions of each compound using $CDCl_3$ or DMSO-d_6 as solvent. Chemical shifts are re- ported in δ units (ppm) with TMS as reference (δ 0.00). All coupling constants (J) are reported in Hertz. Multiplicity is indicated by one or more of the following: s (singlet), d (doublet), t (triplet), q (quartet), m (multiplet). Carbon nuclear magnetic resonance (^{13}C NMR) spectra were recorded on a Brüker at 75 MHz. FT-IR spectra were obtained on a Jasco 4200 spectrometer in KBr discs.

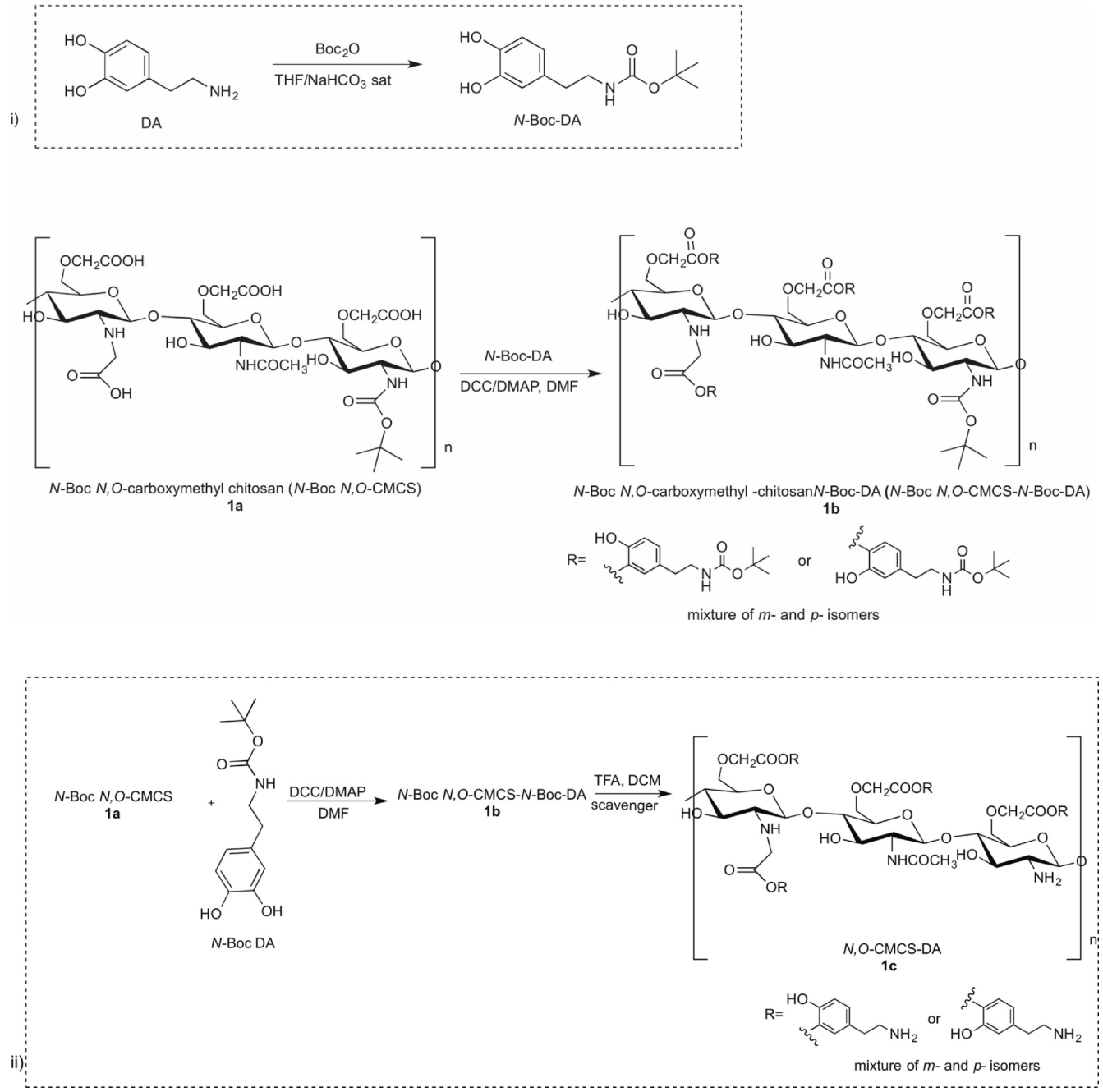

Scheme 1. Synthetic routes for *N*-Boc-DA (panel i) and chitosan derivatives **1c** (panel ii), **1e** (panel iii), and **2c** (panel iv).

2.3. Synthesis of N,O-carboxymethyl chitosan-DA- (Tyr)-conjugates and 6-carboxy chitosan-DA conjugate

*2.3.1. Synthesis of 6-carboxy chitosan (6-carboxyCS **2**)*

The synthesis of *6-carboxyCS* **2** was performed starting from CS (2 g), according to a known procedure already reported for the pre-paration of 6- carboxy cellulose (Klemm et al., 1998). The obtained product (6-carboxyCS **2**) was characterized by FT-IR and ^{1}H NMR. FT-IR (KBr) ν (cm^{-1}): 3435 (OH), 2925, 2855, 2833 (aliphatic CH), 1719 (C▌O) 1362 (OH). ^{1}H NMR (DMSO-d_6) δ (ppm): 11.2 (br s), 5.54 (m), 5.04 (br s), 4.40 (m), 3.50 (m), 3.02 (m), 2.21 (s, *N*-$COCH_3$). Yield: 1.8 g.

The carboxyl group content of the sample was evaluated by the adsorption of methylene blue dye (Klemm et al., 1998) according to the following Eq. (1):

$$mmol\ COOH/g\ dry\ sample = \frac{(7.5 - wf)\cdot 0.00313}{wch} \quad (1)$$

where wf = total amount of free methylene blue in mg and wch = weight of oven-dry sample (g).

*2.3.2. Synthesis of N-tert-butoxycarbonyl N,O-carboxymethyl chitosan (N-Boc N,O-CMCS, **1a**) and N-tert-butoxycarbonyl 6-carboxy chitosan (N-Boc-6-CarboxyCS, **2a**)*

In a 50 mL flask, 1 g of carboxymethyl chitosan or 6-carboxy chitosan was dissolved in 4 mL of ionic liquid [Bmim] [BF_4] (Di Gioia et al., 2014, 2017) and 0.5 mL of water was added as a co-solvent. Di-*tert*-butyl dicarbonate (Boc_2O, 1.047 g, 4.8 × 10^{-3} mol) was then added and left overnight under magnetic stirring at room temperature. At the end of the reaction, the mixture was diluted with diethyl ether (Et_2O) and the ionic liquid, that is immiscible with Et_2O, was settled at the bottom.

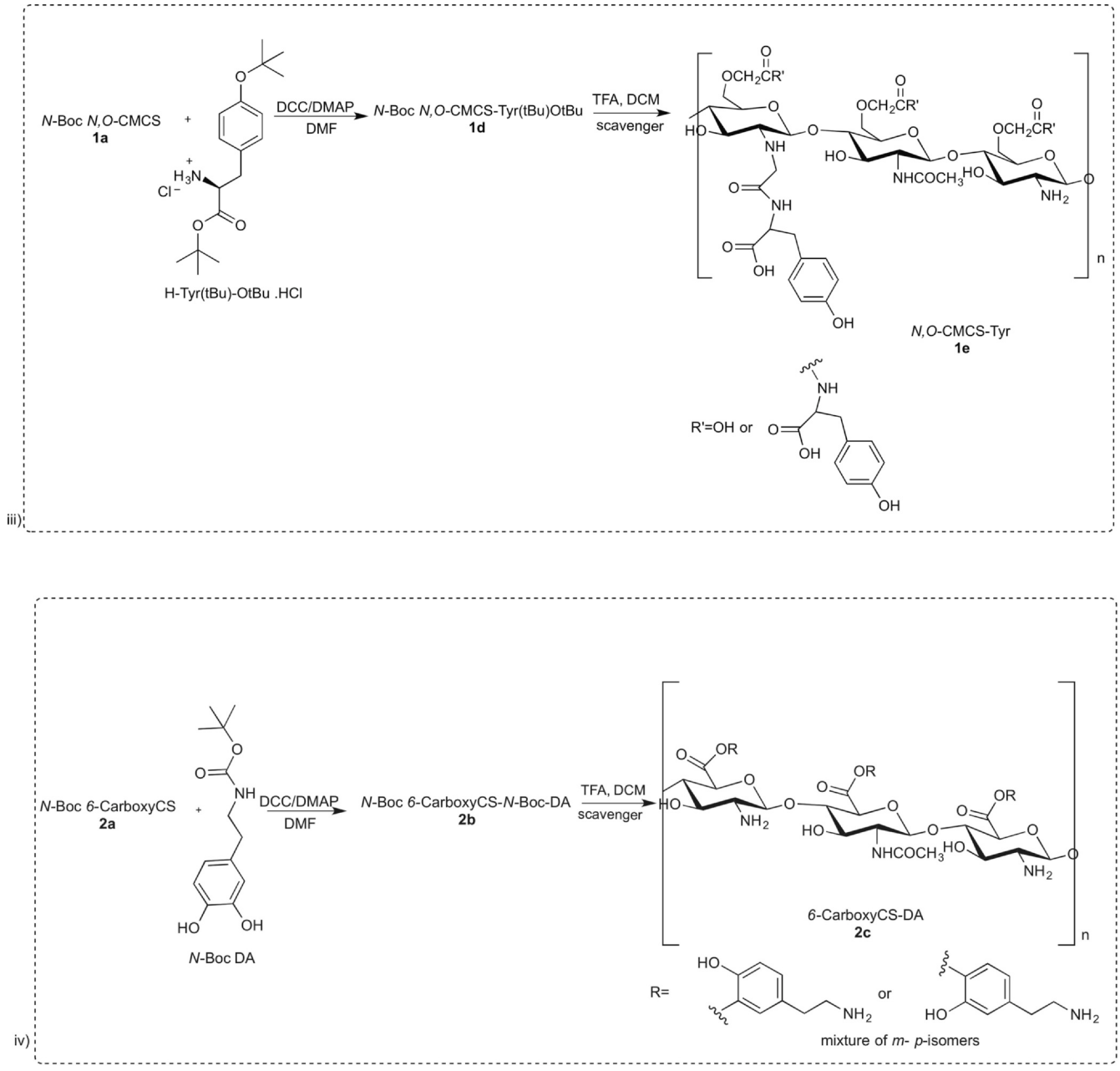

Scheme 1. (*continued*)

After the addition of Et_2O, the formation of a white precipitate was observed. Such precipitate, was filtered and characterized by FT-IR and ^1H NMR analyses as the expected *N*-Boc *N*,*O*-CMCS or *N*-Boc-6-carboxyCS. Even the residue resulting from the evaporation of the dried (sodium sulfate) organic phase (Et_2O) was characterized by FT-IR and ^1H NMR analyses as *N*-Boc *N*,*O*-CMCS or *N*-Boc-6-carboxyCS.

N-Boc *N*,*O*-CMCS **1a**: FT-IR (KBr) ν (cm^{-1}): 3427, 3328 (OH), 2958, 2923, 2854 (aliphatic CH), 1765, 1724 (C▌O) 1380 (OH). ^1H NMR (DMSO-d_6) δ (ppm): 10.8 (br s), 8.13 (d, J = 6.7 Hz), 5.88 (m), 4.40 (m, 2H, CH_2COOH), 4.09–3.55 (m, glucopyranose ring), 3.50–3.21 (m, -N-CH_2COOH), 1.80 (s, N-$COCH_3$), 1.40 (s, $C(CH_3)_3$).

N-Boc-6-carboxyCS **2a**: ^1H NMR (DMSO-d_6) δ (ppm): 11.2 (br s), 8.10 (d, J = 6.7 Hz, NH-$COCH_3$), 7.80 (br s, NH-Boc), 5.90 (m), 4.46 (m, glucopyranose ring), 3.90–3.53 (m, glucopyranose ring), 2.19 (s, N-$COCH_3$), 1.40 (s, $C(CH_3)_3$).

N-Boc-6-carboxyCS **2a**: ^1H NMR (DMSO-d_6) δ(ppm): 11.2 (br s), 8.10 (d, J = 6.7 Hz, NH-$COCH_3$), 7.80 (br s, NH-Boc), 5.90 (m), 4.46 (m, glucopyranose ring), 3.90–3.53 (m, glucopyranose ring), 2.19 (s, N-$COCH_3$), 1.40 (s, $C(CH_3)_3$).

2.3.3. Synthesis of N-tert-butoxycarbonyl dopamine (N-Boc-DA)

In a one-necked flask dopamine hydrochloride (0.86 g) was dis- solved in 10 mL of tetrahydrofuran (THF) and $NaHCO_3$ saturated water solution (5 mL). Then Boc_2O (1.09 g, 1 equiv) was slowly added and left under magnetic stirring at room temperature for 2 h. Then, the reaction mixture was washed with brine, dried over Na_2SO_4, filtered and eva- porated under reduced pressure conditions and the final compound was characterized by FT-IR, ^1H NMR, ^{13}C NMR spectroscopic analyses. *N*- Boc-DA has been prepared following an alternative procedure (Li et al., 2014), but no spectral data have been provided. FT-IR (KBr) ν (cm^{-1}):
3329 (OH), 3068, 3013 (aromatic CH), 2958, 2854 (aliphatic CH), 1724 (C▌O) 1388 (OH). ^1H NMR (DMSO-d_6) δ (ppm): 8.78 (s, 1H, OH), 8.52 (s, 1H, OH), 6.78 (m, NH), 6.57 (d, J = 8 Hz, ArH), 6.50 (s, ArH), 6.38 (d, J = 8 Hz, ArH), 3.12–2.92 (m, 2H, CH_2NH), 2.49 (m, 2H, CH_2Ar)

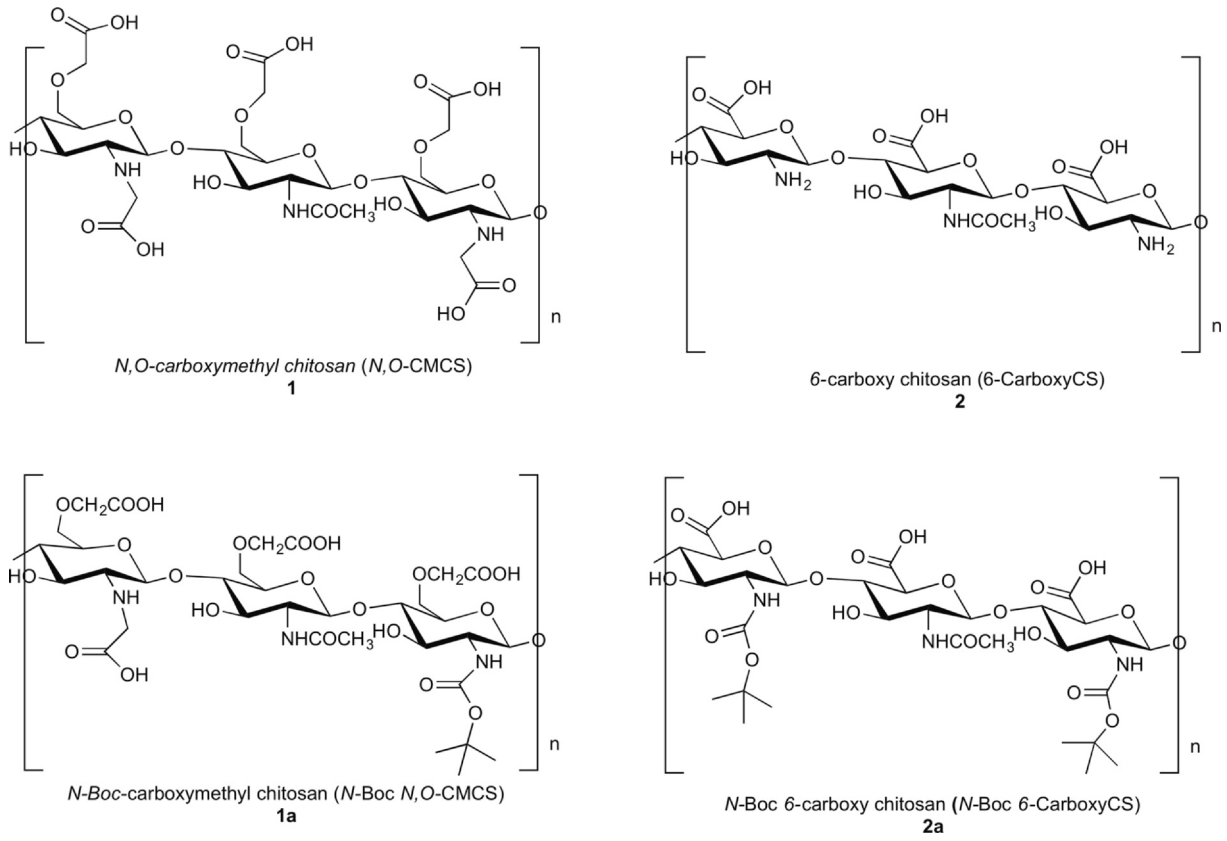

Fig. 1. Chemical structures of *N*,*O*-carboxymethyl chitosan **1** (*N*,*O*-CMCS **1**) , 6-carboxy chitosan **2** (6-carboxyCS **2**) and corresponding *N*-Boc protected polymers (**1a** and **2a**).

1.43 (s, 9H, C(CH_3)$_3$); ^{13}C NMR (DMSO-d_6) δ (ppm): 155.3, 145.4, 143.9, 131.6, 119.6, 115.8, 113.4, 79.8, 39.2, 35.4, 28.7;

2.3.4. *Synthesis of N-tert-butoxycarbonyl N,O-carboxymethyl chitosan-DA conjugate (N-Boc N,O-CMCS-DA conjugate)* ***1b***

To a solution of *N*-Boc protected CMCS **1a** (0.1 g) in DMF, DMAP (0.217 g, 1.77×10^{-3} mol) and DCC (0.146 g, 7.11×10^{-4} mol) were added and left under magnetically stirring for 10 min at 0° C. Then a *N*- Boc DA solution (0.180 g, 7.11×10^{-4} mol) was slowly added and left under magnetic stirring at room temperature overnight. After extrac-tion with diethyl ether, the combined organic phases were subjected to the appropriate washing in order to remove the excess of reagents and dried over sodium sulfate, filtered and the solvent evaporated with a rotary evaporator. The obtained product (*N*-Boc *N*,*O*-CMCS-DA con- jugate **1b**) was characterized by ^{1}H NMR. ^{1}H NMR ($CDCl_3$) δ (ppm): 9.32 (s, OHDA), 8.08 (br s, $NHCOCH_3$), 7.02–6.70 (m, ArHDA, NHDA), 6.52 (m, ArHDA), 4.71–4.60 (m, glucopyranose ring CHOH and OCH_2COOR), 4.40–4.10 (m, OCH_2COOH), 3.65 (m, 2H, N-CH_2COODA), 3.40–3.50 (m, CH anomeric and CH_2 DA), 3.30–3.13 (m, glucopyranose ring CH), 2.80 (m, CH_2 DA), 1.80 (m, $COCH_3$), 1.42–1.38 (br s, C(CH_3)$_3$).

2.3.5. *Synthesis of N-tert-butoxycarbonyl N,O-carboxymethyl chitosan-Tyr conjugate (N-Boc N,O-CMCS-Tyr conjugate)* ***1d***

DMAP (0.87 g, 7.15×10^{-3}mol) and DCC (0.59 g, 2.86×10^{-3}mol) were added to the protected *N*-Boc carboxymethyl chitosan (1 g) solubilized in 10 mL of [Bmim] [BF_4] (Di Gioia et al., 2014, 2017) and left under magnetic stirring for 10 min and at room temperature. O-*t*-Butyl- L-tyrosine *t*-butyl ester hydrochloride (1.77 g, 5.37×10^{-3} mol) was then slowly added and left under magnetic stirring at room temperature overnight. At the end of the reaction, it was extracted with diethyl ether. The combined organic phases were washed to remove the excess of reagents and then dried on sodium sulphate, filtered (with paper filter) and evaporated under reduced pressure. The obtained product was then characterized by FT-IR and ^{1}H NMR. FT-IR (KBr) ν (cm^{-1}): 3435, 3409 (OH), 3110, 3025 (CH aromatics), 2958, 2854 (CH aliphatic), 1790, 1762 (C=O) 1373 (OH). ^{1}H NMR ($CDCl_3$) δ (ppm): 8.13 (d, J = 6.7 Hz, NHAc), 7.17 (d, J = 8.0 Hz, ArH), 6.92 (d, J = 8.0 Hz, ArH), 6.52 (d, J = 6.8 Hz, NHTyr), 4.58 (m, α-CHTyr), 4.22–4.10 (m, OCH_2CO), 3.52–3.40 (m, CH_2O and CH anomeric), 3.30–3.25 (m, CH_2Tyr), 3.20–3.10 (m, glucopyranose ring CH), 1.98 (m, $COCH_3$), 1.40 (s, C(CH_3)$_3$ O*t*Bu protecting group), 1.38 (s, C(CH_3)$_3$ Boc protecting group).

2.3.6. *Synthesis of N-tert-butoxycarbonyl 6-carboxy chitosan-DA conjugate (N-Boc 6-carboxyCS-DA conjugate)* ***2b***

To a solution of *N*-Boc-6-CarboxyCS (0.1 g) in DMF, DMAP (0.20 g, 8.85×10^{-3}mol) and DCC (0.138 g, 3.54×10^{-3} mol) were added under magnetic stirring for 10 min at 0° C. A *N*-Boc DA solution (0.085 g, 3.54×10^{-3} mol) was then slowly added and left under magnetic stirring at room temperature overnight. At the end of the reaction, an extraction with diethyl ether was performed. The combined organic phases were subjected to appropriate washing in order to re- move the excess of reagents. Subsequently after drying over sodium sulfate and filtration the organic solvent was removed by means of rotary evaporator. The obtained product (*N*-Boc 6-CarboxyCS-DA con- jugate) was characterized by ^{1}H NMR. ^{1}H NMR ($CDCl_3$) δ (ppm): 8.12 (br s, $NHCOCH_3$), 8.02 (m, CHNHBoc), 7.00–6.75 (m, ArHDA, NHDA), 6.62 (m, ArHDA), 4.90–4.70 (m, glucopyranose ring CHOH), 3.40–3.10 (m, CH anomeric, CH_2 DA, glucopyranose ring CH), 2.60 (m, CH_2 DA), 1.90 (m, $COCH_3$), 1.42 (br s, C(CH_3)$_3$).

2.3.7. *Removal of Boc protecting groups to give conjugates* ***1c, 1e, 2c***

The final products of the reactions described above (*N*-Boc *N*,*O*-

CMCS-DA-, *N*-Boc *N*,*O*-CMCS-Tyr- and *N*-Boc 6-Carboxy CS-DA-conjugates) were subjected to an acid treatment to remove the corresponding protecting groups. Briefly, the protected products were placed in a reaction flask, trifluoroacetic acid and dichloromethane (50:50) were added in the presence of a scavenger (thioanisole) to block the reactive carbocation formed during the removal of the protecting groups. The mixture was left under magnetic stirring for 2 h. Then, all volatiles were evaporated under reduced pressure and the obtained products were characterized by FT-IR and ^{1}H- NMR.

N,*O-CMCS-DA-conjugate* **1c.** FT-IR (KBr) ν (cm^{-1}): 3546, 3470, 3412 (NH), 3328 (OH), 3124, 3028 (CH aromatic), 2930, 2850 (CH aliphatic), 1723, 1682 (C=O), 1345 (OH). ^{1}H NMR (DMSO-d_6) δ (ppm): 9.00 (s, OHDA), 8.08 (br s, $NHCOCH_3$), 7.02–6.70 (m, ArHDA, NHDA), 6.90–6.50 (m, ArHDA), 4.30–4.10 (m, glucopyranose ring CHOH and OCH_2COOR), 4.00–3.90 (m, OCH_2COOH), 3.68 (m, 2H, N-CH_2COODA), 3.50–3.40 (m, CH_2OCH_2COOH), 3.20–3.10 (m, CH anomeric and CH_2 DA), 3.13–2.90 (m, glucopyranose ring CH),2.70–2.40 (m, $CHNH_2$ glucopyranose ring, CH_2DA), 1.86 (m, $COCH_3$), 1.60–1.50 (m, NH_2 DA, NH_2 CMC).

N,*O-CMCS-Tyr-conjugate* **1e**: FT-IR (KBr) ν (cm^{-1}): 3631, 3592, 3380 (OH), 3160, 3122 (CH aromatics), 2938, 2875 (CH aliphatic), 1729, 1702 (C=O) 1384 (OH). ^{1}H NMR (DMSO-d_6): δ (ppm): 7.37 (d, J = 6.7 Hz, NHAc), 7.07 (d, J = 8.0 Hz, ArH), 6.82 (d, J = 8.0 Hz , ArH), 6.54 (d, J = 6.8 Hz, NHTyr), 4.70 (m, α-CHTyr), 4.22–4.00 (m, OCH_2CO), 3.64–3.40 (m, CH_2O and CH anomeric), 3.30–3.20 (m, CH_2Tyr), 3.19–3.10 (m, glucopyranose ring CH), 2.00 (m, $COCH_3$).

6-CarboxyCS-DA-conjugate **2c**: FT-IR (KBr) ν (cm^{-1}): 3435 (OH), 2925, 2855, 2833 (CH aliphatic), 1719 (C=O) 1362 (OH). ^{1}H NMR (DMSO-d_6) δ (ppm): 8.02 (br s, $NHCOCH_3$), 7.27 (d, J = 8 Hz, ArHDA), 7.02 (s, ArHDA), 6.78 (d, J = 8 Hz, ArHDA), 5.64 (m,), 4.56 (m, glucopyranose ring CH), 3.60 (m, CH anomeric, CH_2 DA), 3.12–2.60 (m, CH_2 DA), 2.03 (m, N-$COCH_3$).

*2.3.8. Determination of substitution degree (DS) of **1c**, **1e** and **2c** conjugates*

To calculate the substitution degree (DS), the *N*,*O*-CMCS-DA- *N*,*O*-CMCS-Tyr- and 6-carboxyCS-DA-conjugates (**1c**, **1e** and **2c**, respec- tively) were subjected to basic hydrolysis (Cassano et al., 2007; Bukzem et al., 2016). Thus, suitable amounts of sample were weighed and dissolved in an ethanolic solution of NaOH 0.25 M. The mixture was kept under stirring at 100 °C for 24 h. Subsequently, a titration with HCl 0.1 N was made using phenolphthalein as pH indicator for the first equivalence point and the methyl red for the second one. The first point is equivalent headline in excess of soda V2 equivalent point; the second equivalent point indicates the neutralization of the acid salt present V1 equivalent point. The moles of hydrochloric acid between the first and the second equivalent point corresponding to the moles of free ester. The DS is, therefore, determined by the following Eq. (2):

$$DS = \frac{MM\ glucose\ unit}{(g\ sample/n\ free\ ester)\text{-}MM\ free\ ester - MM\ H_2O} \quad (2)$$

where n free ester is equal to (V2 equivalent point- V1 equivalent point)·[HCl]; $MM_{glucose\ unit}$ is the molecular mass of glucose unit; g_{sample} the weight of sample; n free ester the mol of free ester; $MM_{free\ ester}$ the molecular mass of free ester and MM_{H2O} the molecular mass of water.

2.4. Quantitative determination of dopamine

The quantitative determination of DA was carried out by HPLC as previously reported (Trapani et al., 2018). Briefly, an HPLC equipment consisting of a Waters Model 600 pump (Waters Corp., Milford, MA), a Waters 2996 photodiode array detector and a 20 μL loop injection particles; Phenomenex, Torrance, CA) column in conjunction with a precolumn C18 insert as a stationary phase and the mobile phase was 0.020 M potassium phosphate buffer (pH 2.8) which eluted in isocratic mode at the flow rate of 0.9 mL/min. Standard calibration curves for DA determination were acquired at 280 nm wavelength dissolving DA in the eluent above mentioned and calibration curve linearity (R^2 > 0.999) was checked over the range of concentrations tested (4.75×10^{-4} to 1.5×10^{-5} M). Upon such conditions DA retention time was 8 min. Data were processed by the EmpowerTM Software.

2.5. Zeta potential measurements

Zeta potentials of the starting polymers and conjugates **1c**, **1e** and **2c** were measured at 25 °C utilizing the Doppler electrophoresis technique performed at 25 °C by a Malvern Nano-ZS instrument (Malvern Instruments, Worcestershire, U.K.). 6-CarboxyCS **2** and all conjugates **1c, 1e** and **2c** were put in water containing 0.05% (v/v) of DMSO to obtain complete (final concentration of 0.1% w/v), whereas *N*,*O*-car- boxymethyl chitosan **1** was dissolved in water as such. Then, in the cuvette, the dilution of each sample was set at 1:20 (v:v) in the presence of KCl (1 mM, pH 7).

*2.6. In vitro evaluation of mucoadhesive properties of **1c**, **1e**, and **2c** conjugates and their corresponding parent polymers*

The mucoadhesive properties of conjugates were evaluated in Simulated Nasal Fluid (SNF) by using an *in vitro* method based on turbidimetric measurements (Trapani et al., 2014). SNF consisted of an aqueous solution containing $CaCl_2$ $2H_2O$ (0.32 mg/mL), KCl (1.29 mg/ mL) and NaCl (7.45 mg/mL) at pH 6.0 (Pagar et al., 2014). Briefly, freshly prepared mucin dispersions at the concentration of 0.5 mg/mL in SNF were maintained at 37 °C under stirring (150 rpm) throughoutthe 24 h of the study. Each conjugate and parent polymer such as *N*,*O*- CMCS **1** and 6-carboxyCS **2** were dispersed in SNF containing 0.05% (v/v) of DMSO to give the final concentration of 0.04% (w/v). In a Falcon tube, to 6 mL of mucin in SNF were added 6 mL of conjugate (or parent polymer) sample. The turbidity of the mixture maintained at 37 °C and under stirring (150 rpm) was measured at 650 nm using a Perkin-Elmer Lambda Bio 20 spectrophotometer at the time points of 7 h and 24 h.HEC dissolved in SNF containing 0.05% (v/v) of DMSO at the concentration of 0.4 mg/mL was taken as control. All experiments were carried out at room temperature in triplicate.

*2.7. Release of dopamine from N,O- carboxymethyl chitosan-DA conjugate **1c** and 6-carboxy chitosan-DA conjugate **2c***

A dispersion of *N*,*O*-carboxymethyl chitosan-DA **1c**- or carboxy chitosan-DA **2c**-conjugate (10 mg) in 1.5 mL of SNF, containing 0.05% (v/v) of DMSO and in absence of enzymes, was thermostated at 37 ± 0.1 °C in an agitated (40 rpm/min) water bath (Julabo, Milan, Italy). At scheduled time-points (0, 1, 2, 3, 8, 17, 24 h), 0.2 mL of the receiving medium were withdrawn and replaced with 0.2 mL of fresh medium. Each sample was centrifuged (16,000 × g, 45 min, Eppendorf 5415D, Germany), and the concentrations of the neurotransmitter were determined in the resulting supernatants by HPLC as above described. For the cumulative release calculation, the approach reported in literature was followed (Tan et al., 2017). All release experiments were carried out in triplicate.

*2.8. Preparation of FITC-N,O-carboxymethyl chitosan **1** and FITC-N,O-carboxymethyl chitosan-DA conjugate **1c***

In view of uptake experiments, *N*,*O*-carboxymethyl chitosan **1** and *N*,*O*-carboxymethyl chitosan-DA conjugate **1c** were labelled with

autosampler (Waters 717 plus) was used. Each chromatographic run was performed by using a Synergy Hydro-RP (25 cm × 4.6 mm, 4 μm

fluoresceine isothiocyanate (FITC) with slight modifications of our previous protocol (Di Gioia et al., 2015). Firstly, CMCS (or *N*,*O*-

carboxymethyl chitosan-DA conjugate **1c**, 100 mg) was dissolved in 1 N HCl (5 mL) and, afterwards, the pH was adjusted to 6.5 with 0.1 N NaOH (4 mL). FITC was dissolved at 20 mg/mL in ethanol and 0.75 mLof this solution were added to the above prepared CMCS (or *N*,*O*-carboxymethyl chitosan-DA conjugate **1c**), solution. The resulting mixture was maintained under stirring at room temperature for 24 h and protected from light. Then, the mixture was dialyzed against double distilled water using dialysis tubes for 3 days and freeze dried for 72 h (Lio Pascal 5P, Italy). To determine the labelling efficiency of FITC-CMCS, the fluorometer (Perkin Elmer, Italy) was calibrated in the range 1–140 ng/mL of FITC prepared by diluting 100 μg/mL of a methanolic solution of FITC with phosphate buffer at pH 8.0 (excitation wavelength: 488 nm; emission wavelength: 525 nm; slits: 2.5 nm). Labelling efficiency of FITC-CMCS (or FITC- *N*,*O*-carboxymethyl chitosan-DA conjugate **1c**) was defined as percentage of mass FITC/mass FITC-CMCS (or FITC- *N*,*O*-carboxymethyl chitosan-DA conjugate **1c**).

2.9. Cytotoxicity studies with olfactory Ensheathing cells (OECs)

Experiments were performed on 2-day-old mouse pups (P2, provided by Envigo RMS s.r.l. Italy, stock: C57BL6J). Animals were kept in a controlled environment (23 ± 1 °C, 50 ± 5% humidity) with a 12 h light/dark cycle with food and water available ad libitum. Experiments were carried out in compliance with the Italian law on animal care no. 116/1992 and in accordance with the European Community Council Directive (86/609/EEC). Efforts were made to minimize the number of animals used. OECs were isolated from mouse P2 olfactory bulbs, and cultured in DMEM/FBS as previously described (Musumeci et al., 2014). After 24 h the antimitotic agent, cytosine arabinoside (10^{-5} M), was added to reduce the number of dividing fibroblasts. Then, OECs were plated on 25 cm^2 flasks and cultured in DMEM/FBS supplemented with a bovine pituitary extract. Cells were incubated at 37 °C in a fresh complete medium and were fed twice a week. Successively, OECs were plated at the number of 30,000 per each well of a 96-well plate. Cells were incubated with either DA, CMCS-DA conjugate **1c**, CarboxyCS-DA conjugate **2c**, CMCS-Tyr-conjugate **1d** (200 μL, 50 μL, 12.5 μL, 3.12 μL, 0.78 μL of an initial stock solution of 75 μM), *N*,*O*-CMCS or 6-CarboxyCS (200 μL, 50 μL, 12.5 μL, 3.12 μL, 0.78 μL) in complete medium. After 24 h, cells were tested for viability by the 3-(4,5-dimethylthiazol-2-yl)-2,5 diphenyl tetrazolium bromide (MTT) assay, as previously described (Di Gioia et al., 2015). The relative viability was calculated in respect to control untreated cells (considered as 100%). 1% SDS-treated cells were used as positive control.

2.10. Uptake studies

OECs were plated at the number of 50,000 per each well of a 24-well plate. Cells were incubated with either FITC-DA-CMCS **1c** (500 μL or 125 μL of an initial stock solution of 75 μM DA) or FITC-CMCS (500 μL or 125 μL of an initial stock solution containing an amount of CMCS corresponding to that used in the DA conjugates) in complete medium. After 2 or 24 h, each well was treated with 0.04% trypan blue in PBS (in order to quench extracellular fluorescence), trypsinized, resuspended in 0.5 mL of PBS, and analysed by the Attune® NxT Acoustic Focusing Cytometer (ThermoFisher Scientific, Life Technologies, Monza, Italy). The percentage of positive cells was obtained by gating the population of interest, accordingly to previously published protocols (Leme Silva et al., 2018) and detecting the emission of FITC signalin the BL1 channel (530/30 nm). The percentage of positive cells was determined setting the gating on 99% of an untreated control population of cells and by subtracting their fluorescence. Ten thousand cells were examined in each analysis.

2.11. Statistical analysis

Statistical analyses were carried out by Prism Version 4, GraphPad Software Inc., USA. Data were expressed as either mean ± SD. Multiple comparisons were based on One-way Analysis of Variance (ANOVA) with the either Bonferroni's or Tukey's post hoc test and differences were considered significant when $p < 0.05$.

3. Results

6-carboxyCS **2** was synthesized being commercially unavailable, unlike *N*,*O*-CMCS **1**. It was prepared by $H_3PO_4/NaNO_2$ mediated oxi- dation of the primary hydroxyl group on C6 of glucosamine units of CS, adapting a method already reported in literature for the oxidation of the primary hydroxyl group on C6 of D-glucopyranose moieties in cellulose (Cassano et al., 2009, 2010). Thus, 6-carboxyCS **2** was characterized by FT-IR and ^{1}H NMR spectral analyses (see section 2.3.1.). In particular, the corresponding FT-IR spectrum shows two characteristic absorption bands at 3435 and 1719 cm^{-1}, the former attributable to the stretching of the OH bond and the latter due to the stretching vibration of the C=O double bond. In the relative ^{1}H NMR spectrum recorded in DMSO-d_6, the broad signal at 11.2 ppm was assigned to –OH of the carboxyl group. The determination of the carboxyl group content in **2** was as-sessed by methylene blue adsorption technique in which the cation moiety of methylene blue binds with anionic carboxylic groups (Jabliand Hassine, 2018). In such a way, the content of carboxyl groups in the synthesized derivative **2** resulted equal to 0.54 mmol COOH/g oven-dry 6-CarboxyCS.

*3.1. Synthesis and characterization of conjugates **1c**, **1e** and **2c***

As shown in Scheme 1, DCC mediated coupling reactions between the appropriate *N*-Boc protected polymer **1** or **2** and *N*-Boc-DA or Tyr (OtBu)-OtBu HCl were employed to prepare the corresponding con- jugates **1b, 1d** and **2b.** It is noteworthy that the preparation of *N*-Boc *N*,*O*-CMCS, *N*-Boc-6-CarboxyCS and *N*-Boc *N*,*O*-CMCS-Tyr conjugate **1d** was carried out in [Bmim] [BF_4] which allowed for the *tert*-butyloX- ycarbonylation of the amino group under very mild conditions (Di Gioia et al., 2014, 2017), whereas in the remaining cases such treatment with ionic liquid was unnecessary. It should be also mentioned that the usefulness of *tert*-butoxycarbonyl as a protecting group in the synthesis of dopamine derivatives is well known since long time (Walker et al., 1978). Next, the nitrogen-protecting group, *i.e.*, the *tert*-butoxycarbonyl moiety, was easily removed by treatment with TFA in DCM and in the presence of thioanisole as a scavenger to give the corresponding conjugates **1c, 1e** and **2c.** These conjugates were structurally characterized on the basis of FT-IR and ^{1}H NMR spectroscopic analyses (see section 2.3.7.). In particular, conjugates **1c** and **2c** showed in their FT-IR spectra a characteristic absorption band at 1723 cm^{-1} and 1719 cm^{-1}, respectively, attributable to ester carbonyl. Moreover, the corre- sponding ^{1}H NMR spectra showed the characteristic signals attributable to the protons in *orto* and *meta* positions of the aromatic ring of DA occurred in the range 7.3–6.5 ppm. Fig. S1 shows the ^{1}H NMR spectra of *N-Boc* DA, the *N*-Boc *N*,*O*-CMCS-DA conjugate **(1b)** and, lastly, the ^{1}H NMR spectrum of **1c**.

The DS of conjugates **1c**, **1e** and **2c** was determined by acid-base volumetric titration employing two pH indicators as described in section 2.3.8. Briefly, an excess of ethanolic solution of NaOH was used to hydrolyze the conjugate. The excess of NaOH was determined by a titration with HCl using phenolphthalein as pH indicator while methyl red was used for the neutralization of the acid salt present (Cassano et al., 2007; Bukzem et al., 2016). In this way it resulted that the DS values of **1c**, **1e** and **2c** were 100 mg and 140 mg of DA for **1c** or **2c** conjugate (1 g) as well as 52 mg of Tyr for **1e** conjugate (1 g), respectively.

Both starting polymers (**1** and **2**) and conjugates **1c**, **1e** and **2c** are characterized by a polyanionic structure. It is confirmed by the zeta potentials of these macromolecules which resulted negative values inthe range from −18.4 mV to −42.6 mV (Table 1). These findings can

Table 1
Zeta potentials of the starting polymers **1** and **2** and conjugates **1c**, **1e** and **2c**.

Polymer	Zeta Potential (mV)
1	−20.7 (± 1.5)
2	−21.8 (± 2.0)
1c	−18.4 (± 2.6)
1e	−32.7 (± 2.6)
2c	−42.6 (± 1.1)

be accounted for taking into account that the starting carboxylated chitosans as well as the corresponding conjugates are in the $eCOO^-$ form since the zeta potential measurements have been performed at pH 7, where complete dissociation of eCOOH groups should occurs together with the deprotonation of the amino groups of the CS derivatives herein evaluated.

3.2. *In vitro evaluation of mucoadhesive properties of conjugates **1c**, **1e** and **2c** and their parent polymers*

The mucoadhesive properties of the conjugates **1c**, **1e** and **2c** and their parent polymers were determined *in vitro* by turbidimetric measurements using mixtures of each of these macromolecular substances in SNF containing little amount of DMSO [0.05% (v/v)] to allow their complete dispersion. As known, by mixing such mixtures with mucin dispersions in the same medium, an incubation time-dependent decrease in transmittance occurs consequent to polymer-mucin aggregates formation (Rossi et al., 2000). An incubation time of 24 h seemed appropriate to compare the mucoadhesive properties of the macromolecular substances examined with those of HEC included herein as positive control and endowed with good mucoadhesive characteristics (Ivarsson and Wahlgren, 2012).

As shown in Fig. 2, essentially both the parent polymers and the majority of the macromolecular substances examined were characterized by mucoadhesive properties comparable with those of HEC. However, the highest decrease in transmittance after 24 h of incubation time was observed for *N*,*O*-CMCS-DA conjugate **1c** which resulted in statistically significant difference ($p < 0.01$) *vs* HEC. It is worth to notice that the differences between *N*,*O*-CMCS-DA conjugate **1c** *vs* CarboxyCS-DA **2c** and *N*,*O*-CMCS-Tyr **1e** were also statistically significant ($p < 0.05$ and $p < 0.001$, respectively). Instead, the differences in transmittance decrease between parent polymers, *N*,*O*-CMCS-Tyr **1e** and HEC were not significant.

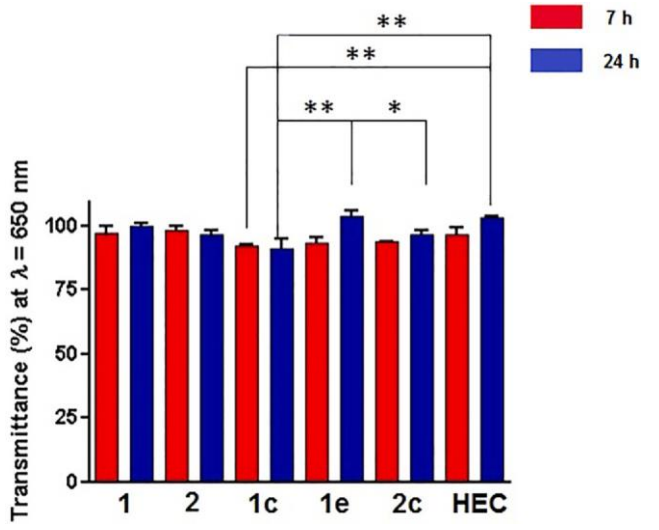

Fig. 2. Mucoadhesive properties of *N*,*O*-CMCS **1**, carboxyCS **2** and their conjugates **1c**, **1e** and **2c** in SNF. HEC in the same medium was taken as positive control and considered as 100%. Incubation time of 7 h (red bars) and 24 h (blue bars). * $p < 0.05$ *vs* control; ** $p < 0.01$ *vs* control.

Hence, it seems that the rank order of the polymers examined from the mucoadhesive properties point of view is the following: *N*,*O*-CMCS-DA **1c** > CarboxyCS-DA **2c** > *N*,*O*-CMCS **1**, CarboxyCS **2**, *N*,*O*-CMCS-Tyr **1e** ~ HEC. However, it should be mentioned that visual inspection of CMCS-DA conjugate **1c** after 24 h of incubation time showed that this sample turned to black colour, while this did not occur for the same sample after 7 h of incubation. The colour change observed should be due to the spontaneous autoxidation of free DA formed by hydrolytic cleavage in SNF of this ester conjugate **1c** and/or to the oxidative instability of the entire conjugate (Trapani et al., 2018).

3.3. *Dopamine release from conjugates **1c** and **2c** in simulated nasal fluid*

To evaluate whether conjugates **1c** and **2c** can undergo chemical hydrolysis to give the neurotransmitter directly in the simulated nasal electrolyte solution, release studies were carried out in SNF without enzymes at pH 6. These conjugates were selected because of their mucoadhesive properties better than HEC. The results obtained are shown in Fig. 3 from which it can be seen that about 43% of DA was released in 3 h from conjugate **2c**, while only about 15% of DA wasreleased in 3 h from conjugate **1c**.

3.4. *Polymers **1**,**2** and conjugates **1c**, **1e**, **2c** were non-toxic to OECs*

In order to see whether either the parent polymers or their conjugates were toxic in their way to the olfactory bulb, polymers or conjugates were incubated with OECs and cell viability was assessed after 24 h by the MTT assay. As shown in Fig. 4, parent polymers (*N*,*O*- CMCS and CarboxyCS), as well as DA, were not toxic to OECs at any concentration tested as compared with the appropriate control (untreated cells). The three conjugates **1c**, **1e** and **2c** were not cytotoxic as well.

3.5. *Enhanced uptake by OECs of DA-conjugates compared with the parent polymers*

For uptake studies fluorescent *N*,*O*-CMCS **1** and *N*,*O*-CMCS-DA **1c** were prepared by covalent linkage of FITC (labelling efficiency of 56 μg FITC/mg di FITC-CMCS **1** and 75 μg FITC/mg di FITC-CMCS **1c**, respectively). Cell uptake was studied in OECs following incubation for either 2 or 24 h. Fig. 5a and b illustrate the cytofluorimetric gating and analysis made on the total population that have been used for each condition. Gated cells (Fig. 5a) were evaluated for fluorescence intensity (Fig. 5b), that is then shown in Fig. 5c as histograms. As expected, the uptake was a time-dependent process with more polymers internalised at 24 h than at 2 h. Moreover, it can be appreciated that

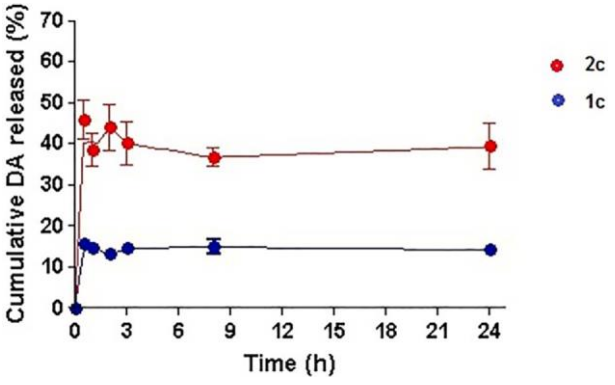

Fig. 3. DA released from conjugate **1c** (blue) and **2c** (red).

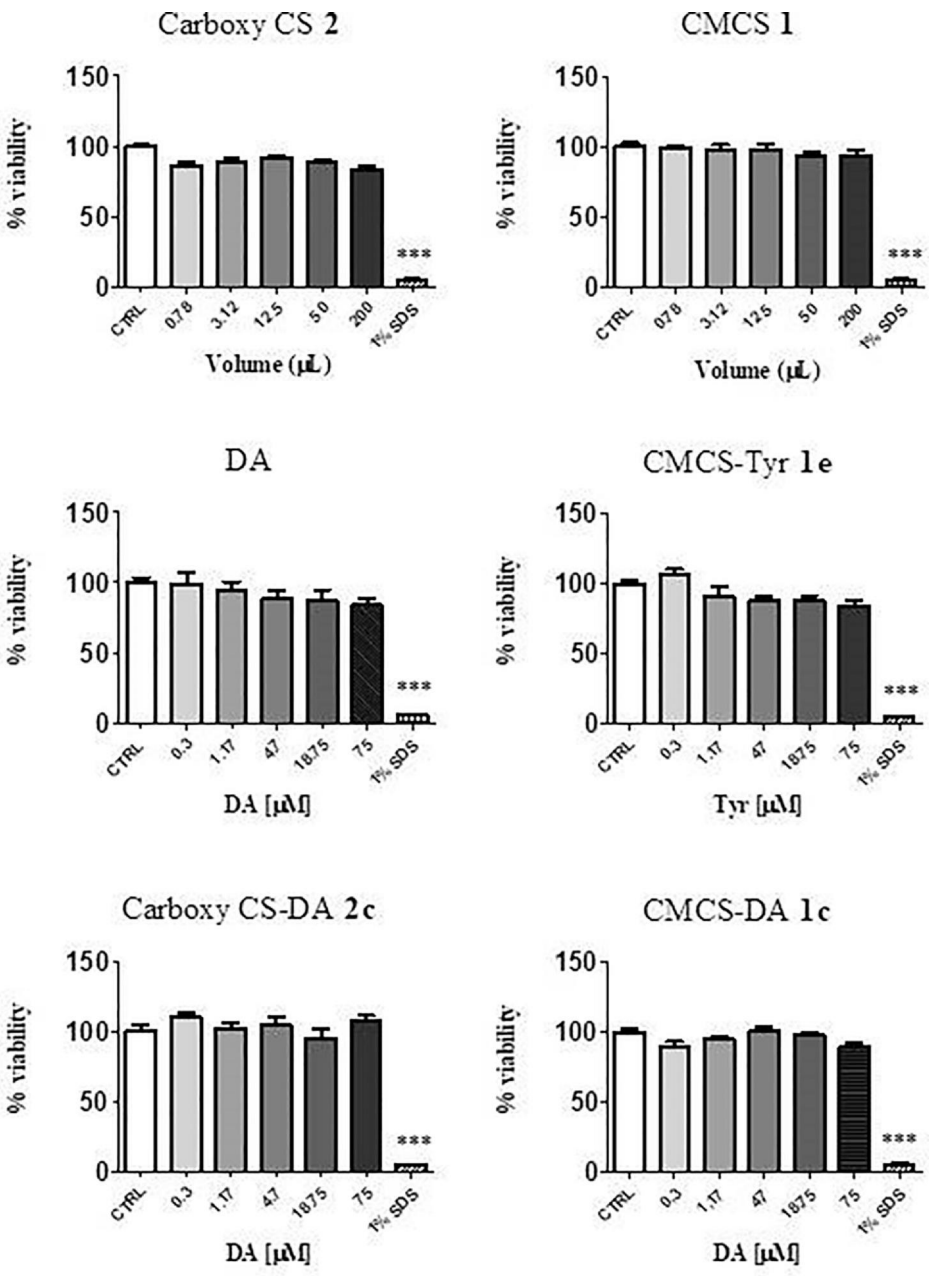

Fig. 4. Cytotoxicity of polymers and conjugates. OECs were challenged with *N*,*O*-CMCS **1** or carboxyCS **2** for 24 h at the indicated volumes. DA and conjugates **1c**, **1e** and **2c** were used at equivalent volumes and obtaining the indicated DA or Tyrosine (Tyr) concentrations. Cells were then assayed for vitality by the MTT assay. Controls (CTRL) are untreated cells (100% of vitality), whereas 1% SDS refers to positive controls. ***$p < 0.0001$ *vs* control. Data are the results of two-three experiments each carried out in six wells.

CMCS-DA **1c** was internalised by OECs in higher amounts than the parent polymer CMCS **1** and at both the doses tested. However, these differences resulted significant only at 24 h with the highest dose. In- terestingly, this dose of CMCS-DA (75 μM) gave a significant increase in the uptake at 24 h when it was compared with the earlier time point of 2 h. Overall, these results strongly indicate that the uptake by OECs istime and dose-dependent and also that the DA moiety gives up some advantage to the internalization process.

4. Discussion

The aim of this work was to prepare, characterize and assess the *in vitro* toxicity and uptake from olfactory bulb-derived cells of carboxy- lated chitosan-dopamine or -tyrosine conjugates **1c**, **1e** and **2c** (Scheme 1) and evaluate their potential for a nose-to-brain DA delivery. It should be considered that these macromolecular conjugates, as other already known polymeric conjugates of the neurotransmitter, may be also administered as nanostructured carriers, unlike analogous DA conjugates with low molecular weight moieties (Denora et al., 2012). Therefore, we designed some carboxylated chitosan-dopamine or -tyrosine con- jugates linked by an ester or amide group, exploiting the –COOH function of the carboxylated chitosans and the eOH groups of the neurotransmitter DA or the eNH_2 group of Tyr. Hence, ester conjugates **1c** and **2c** are actually mixtures of *m*- and *p*-isomers, since each of the catechol hydroxyl groups of DA can be involved in the ester bond formation, just as reported in Scheme 1. In the case of the *N*,*O*-CMCS-Tyrosine conjugation, the synthetic approach involving the use of *O*- *tert*-Butyl-L-tyrosine-*tert*-butyl ester hydrochloride led to the formation of the amide conjugate **1e** (Scheme 1, panel iii)).

Taking into account that polymers having mucoadhesive properties

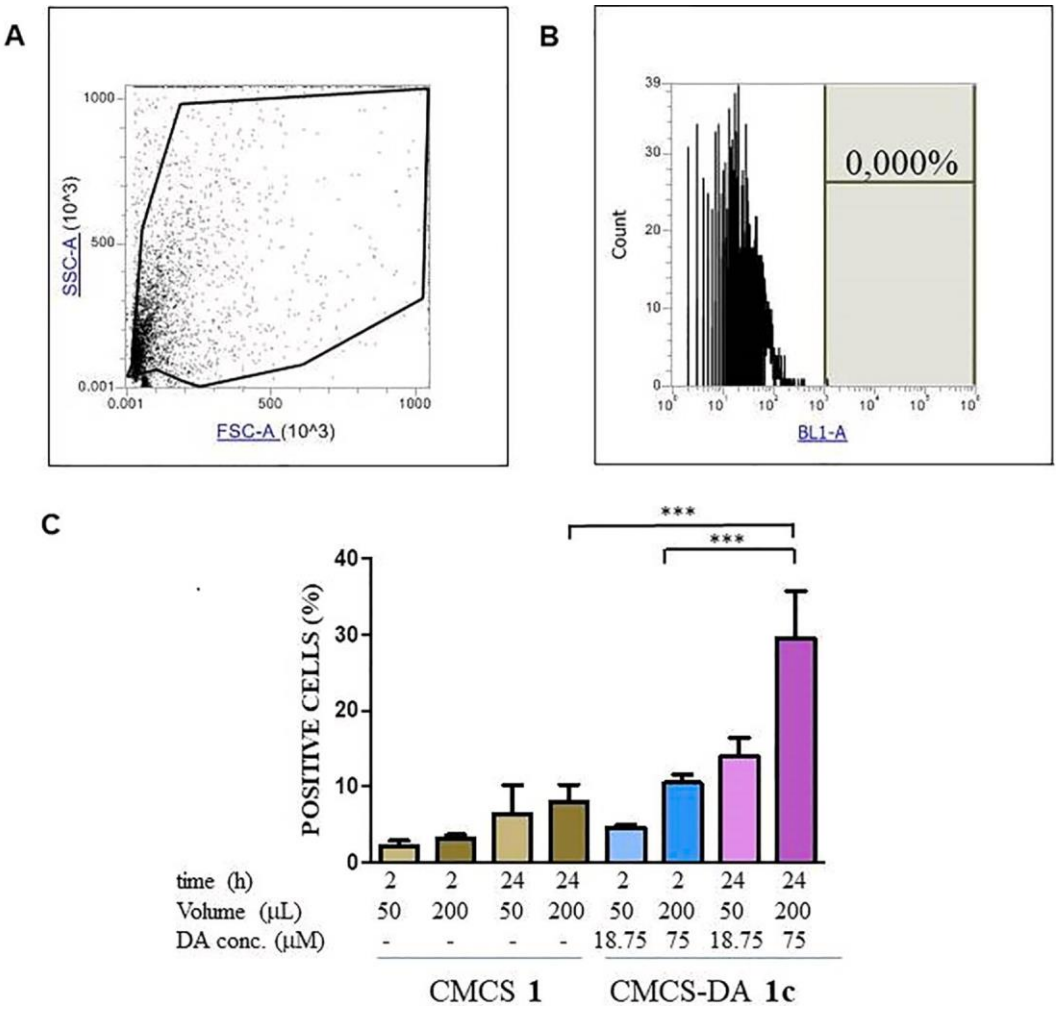

Fig. 5. Cellular uptake of FITC-CMCS **1** or FITC-CMCS-DA **1c** by OECs. The whole population of controls (cells not incubated with polymers) was gated (A) and evaluated for fluorescence intensity (B). A marker separated negative cells (on the left) from positive cells (on the right). Positive cells are shown as percentages (C) obtained in two experiments each conducted in triplicate. ***$p < 0.001$.

can be positively employed in nose-to-brain delivery since they can increase the residence time in the nasal cavity improving absorption of pharmaceutics (Bourganis et al., 2018; Samaridou and Alonso, 2018),we measured such properties for conjugates **1c**, **1e** and **2c** and their parent polymers using HEC as a positive control (Trapani et al., 2014). To account for the rank order observed for the mucoadhesive properties of the mentioned macromolecules (Fig. 2), first of all it should be noted that among the polymer structural characteristics required for in- creasing the mucoadhesive properties there are the presence of strong hydrogen bonding groups (eOH, eCOOH), strong cationic or anionic charges, high molecular weight and appropriate chain flexibility (Mandracchia et al., 2017b; Palazzo et al., 2017). Both **1** and **2** are characterized by the presence of a large number of hydroxyl and car- boxyl groups able to interact with the hydroxyl groups of mucin. Moreover, due to the presence of carboxyl groups which are ionized on increasing the pH of the medium, both **1** and **2** possess a polyanionic structure. This structural feature occurs also for the conjugates **1c**, **1e**and **2c**. Hence, the mucoadhesive properties of the parent polymers and conjugates should be ascribed to hydrogen bonding interactions with the negatively charged mucin. As for the choice of HEC as a positive control for mucoadhesion measurements, it was based on the following reasons. Firstly, Carbopol, which is a well known reference polymer for *in vitro* mucoadhesion tests (Ivarsson and Wahlgren, 2012), could not be used throughout this study due to the fact that it precipitates in SNF. Moreover, HEC surface charge is essentially close to the neutrality (Smistad et al., 2017) but its mucoadhesive properties are consequent to hydrogen bonding interactions with mucin as well as polymers **1** and **2** and conjugates **1c**, **1e** and **2c**. These circumstances are different at all from those occurring between CS and mucin. In this last case, indeed, the interactions between the polycation CS and the negatively charged mucin are mainly electrostatic in nature (Sogias et al., 2008; Ancona et al., 2014). Besides this, another recent literature suggestion, that should be taken into account to explain the mentioned mucoadhesive properties rank order, is that polymer mucoadhesion can be sig- nificantly improved by introduction of catechol moieties in the chain backbone of CS (Kim et al., 2015). This enhancement of mucoadhesive properties should be ascribed to intermolecular associations of the ca- techol group grafted on CS to mucin in the first stage of the mu- coadhesion process (*i.e.*, the so called contact stage). Such initial in- teractions are followed by the formation of covalent bonds between catechol group of the CS and amine/cysteine moieties of mucin leading to irreversible bonds in the second stage of the mucoadhesion process (*i.e.*, the so called consolidation stage) with enhancement of mu- coadhesion up to more than four-fold (Kim et al., 2015). In the CS-derivatives-DA conjugates herein examined, namely *N*,*O*-CMCS-DA conjugate **1c** and 6-CarboxyCS-DA conjugate **2c**, a modified catechol group is present being one hydroxyl group of DA involved in an ester bond formation. As a consequence, it may be possible that the men- tioned structural characteristics lead to moderate enhancement in mucoadhesion for conjugates **1c** and **2c**, whereas this should not occur

for **1e**, due to the absence of a catechol group. Hence, the findings that the mucoadhesion of **1c** and **2c** was better than HEC, while that of **1e** was comparable with those of HEC, *N*,*O*-CMCS and 6-CarboxyCS, may be so accounted for. The mucoadhesive features observed for **1c** better than **2c** may be rationalized considering the flexibility of the former conjugate due to the presence of the carboxymethyl groups linked at C- 6 of the glucosamine units of the CS structure greater than that of 6- Carboxy moiety of the latter conjugate. Thus, the mucoadhesive prop- erties of **1c**, deduced by turbidimetric measurements, suggest that this conjugate may be usefully applied for nose-to-brain delivery of the neurotransmitter DA. However, it is widely recognized that, in the as- sessment of mucoadhesive properties for the ranking of polymers by *in vitro* methods, caution should be used since conflicting results can be obtained depending on the method employed (Ivarsson and Wahlgren, 2012). Therefore, there is a need to confirm such *in vitro* results based on turbidimetric measurements with *in vivo* experiments before to draw definitive conclusions.

As for the DA release from conjugates **1c** and **2c** in SNF without enzymes, it should be pointed out that the purpose of this *in vitro* study was to evaluate whether conjugates **1c** and **2c** can undergo chemical hydrolysis in simulated nasal electrolyte solution to give the neurotransmitter, independently of that resulting from enzyme-mediated hydrolysis. The obtained results indicate that both conjugates can be converted into DA, even though at different extent, by chemical hydrolysis. In our opinion, the relevant difference in DA released between the two conjugates may be ascribed once again to the greater flexibilityof conjugate **1c** compared to **2c**. This last is characterized by a more constrained and rigid structure which is lighten by hydrolysis of the corresponding ester function releasing the neurotransmitter DA. Hence, the tendency of conjugate **2c** to undergo hydrolytic ester bond cleavage is greater than conjugate **1c**. However, the low DA amount released from conjugate **1c** may be even advantageous for nose-to-brain delivery of the neurotransmitter because of a potential decrease in neuronal toxicity related to the reduced stimulation of dopaminergic neurons (Kura et al., 2013). On the other hand, DA as neurotransmitter is a potent substance and its biological effects occurs even if present in little amount. However, to gain useful information on the release features, *in vivo* studies on these conjugates are mandatory. Finally, by comparingthe release kinetic of poly(aspartamide) based DA conjugates (Juriga et al., 2018) with that herein observed for conjugates **1c** and **2c**, it resulted that the poly(aspartamide) based DA conjugates provided prolonged drug delivery, unlike conjugates **1c** and **2c** which show an initial prompt neurotransmitter release. We believe that such outcome may be related to the different linkage involved in the conjugates herein considered. More precisely, in poly(aspartamide) based DA conjugates the neurotransmitter is linked to the polymeric chain through an amide bond, which is more resistant to hydrolytic cleavage, unlike the ester conjugates **1c** and **2c**.

In light of a nose-to-brain administration of DA-containing conjugates, it should be considered that the intranasal route would havethe advantage of bypassing the BBB offering a noninvasive and effective treatment of Central Nervous System (CNS) disorders. When the drug is administered into the nasal cavity, it firstly experiences the mucociliary clearance in the vestibular region, hence the property of mucoadhesion would limit the mucociliary clearance of the drug. Afterward, the drug moves to the posterior region of nasal cavity where it comes in contact with the olfactory region. At this level, the drug would interact with the endings of olfactory receptor neurons and is then transported through the brain following the nerve channel created by OECs, crosses the cribriform plate and enters into the cerebrospinal fluid and olfactorybulb (Agrawal et al., 2018). Thereby, the lack of cytotoxicity of poly-mers and derived conjugates experienced in our results are in good achievement of a safe transport of these compounds. Interestingly, polymer CMCS **1** and its derivative CMCS-DA were internalized by OECs very poorly after 2 h, while only the CMCS-DA conjugate achieved around 30% of positive cells at 24 h. Why the presence of DA confers such an advantage may be inferred from the heightened uptake of various nanoparticles when coated with polydopamine (PDA) (Liu et al., 2013; Poinard et al., 2019). It was suggested that the enhanced uptake of these nanoparticles could be due to their hydrophilicity and the interaction of the negatively charged phenol groups on the PDA surface with the positively charged choline groups on the lipid mem- brane (Liu et al., 2013). In alternative, it has been proposed that do- pamine transporter (DAT) occurs in olfactory bulb (Cockerham et al.,2016) suggesting that the CMCS-DA conjugate **1c** may be also a DAT substrate, however the expression of DAT should be investigated further in primary OECs used in this study. It is worth noting that OECs have been considered a promising source of cell-based therapies for neuro- degenerative disorders (Pellitteri et al., 2016). OECs have been used because they are able to secrete trophic factors with neuroprotective effects and to promote plasticity in the lesioned area (Franssen et al., 2007). For example, axon regeneration in CNS injury site has been imputed to neurotrophin secretion and to conduit formation that ex- press extracellular matrix proteins that have been shown to directly promote neuronal survival, neurite initiation and axon extension, and particularly axonal guidance (Yang et al., 2015). OECs in the olfactory bulb, if loaded with DA *in situ*, might be considered to represent a source that is therapeutic at different levels, including the safe deliveryof DA for the PD.

5. Conclusions

Carboxylated chitosan-dopamine or -tyrosine conjugates **1c, 2c** and **1e** were successfully synthesized and characterized by FT-IR and ^{1}H-and ^{13}C NMR analyses. Moreover, these new chitosan derivatives were evaluated in SNF for their mucoadhesive properties and results showed that the polymers examined can be classified from the mucoadhesive properties point of view in the following rank order: *N*,*O*-CMCS-DA **1c** > CarboxyCS-DA **2c** > *N*,*O* CMCS, CarboxyCS, CMCS-Tyr **1e** ~ HEC. As for the neurotransmitter DA release, *in vitro* studies showed that both the conjugates **1c** and **2c** give rise in SNF to a prompt neurotransmitter release being the DA amount released from conjugate **1c** lower than **2c**. These peculiar features may be advantageous in apotential their application for PD treatment. In this study, we chose OECs as belonging to olfactory system which is the first to show deficitin some neurodegenerative diseases, such as PD. The cytotoxicity of conjugates **1c, 2c** and **1e** assessed on OECs resulted negligible, and this would demonstrate their good biocompatibility and possible applica- tion for nose-to-brain delivery. Moreover, the uptake of conjugate **1c** would be promising to generate a novel tool for delivering DA to the brain.

Overall, the results of these studies suggest that the carboxylated chitosan-dopamine conjugate **1c** possess an interesting potential for improving the brain delivery of the neurotransmitter DA following nasal administration. Further studies are in progress to assess the *in vivo* performance of this conjugate and the corresponding results will be reported in due course.

CRediT authorship contribution statement

Roberta Cassano: Project administration, Writing - original draft. **Adriana Trapani:** Conceptualization, Project administration, Writing - review & editing, Supervision. **Maria Luisa Di Gioia:** Funding acquisition, Methodology. **Delia Mandracchia:** Investigation, Data curation. **Rosalia Pellitteri:** Investigation, Software, Methodology. **Giuseppe Tripodo:** Validation, Visualization. **Sonia Trombino:** Funding acquisition, Methodology. **Sante Di Gioia:** Conceptualization, Formal analysis, Investigation. **Massimo Conese:** Conceptualization, Validation, Methodology.

Declaration of Competing Interest

The authors declare that they have no known competing financial interests or personal relationships that could have appeared to influ- ence the work reported in this paper.

Acknowledgements

This work was partially financed by University of Bari (Italy) to A.T. (Cod. CUP:H91J11000160001) and by Department of Pharmacy and Health and Nutrition Sciences- UniCal (CS), Italy -Department of Excellence-Law 232/2016 to R.C. and M.L. Di Gioia. S.D.G and M.Cwould also acknowledge Antonio Minò and Simona de Nittis (University of Foggia, Italy) for their valuable technical assistance.

Appendix A. Supplementary material

Supplementary data to this article can be found online at

References

Agrawal, M., Saraf, S., Saraf, S., Antimisiaris, S.G., Chougule, M.B., Shoyele, S.A., Alexander, A., 2018. Nose-to-brain drug delivery: An update on clinical challenges and progress towards approval of anti-Alzheimer drugs. J. Control Release 281, 139–177. Available from https://www.ncbi.nlm.nih.gov/pubmed/29772289. DOI 10.1016/j.jconrel.2018.05.011.

Ancona, A., Sportelli, M., Trapani, A., Picca, R.A., Palazzo, C., Bonerba, E., Mezzapesa, F., Tantillo, G., Trapani, G., Cioffi, N., 2014. Synthesis and characterization of hybrid copper-chitosan nano-antimicrobials by femtosecond laser-ablation in liquids. Mater. Lett. 136, 397–400.

Anitha, A., Divya Rani, V.V., Krishna, R., Sreeja, V., Selvamurugan, N., Nair, S.V., Tamura, H., Jayakumar, R., 2009. Synthesis, characterization, cytotoxicity and antibacterial studies of chitosan, *O*-carboxymethyl and *N*, *O-carboxymethyl chitosan nanoparticles*. Carbohydr. Polym. 78 (4), 672–677.

Bonengel, S., Bernkop-Schnurch, A., 2014. Thiomers–from bench to market. J. Control Release 195, 120–129. Available from https://www.ncbi.nlm.nih.gov/pubmed/24993428. DOI 10.1016/j.jconrel.2014.06.047.

Bourganis, V., Kammona, O., Alexopoulos, A., Kiparissides, C., 2018. Recent advances in carrier mediated nose-to-brain delivery of pharmaceutics. Eur. J. Pharm. Biopharm. 128, 337–362. Available from https://www.ncbi.nlm.nih.gov/pubmed/29733950. DOI 10.1016/j.ejpb.2018.05.009.

Bukzem, A.L., Signini, R., Dos Santos, D.M., Liao, L.M., Ascheri, D.P., 2016. Optimization of carboxymethyl chitosan synthesis using response surface methodology and desirability function. Int. J. Biol. Macromol. 85, 615–624. Available from https://www.ncbi.nlm.nih.gov/pubmed/26778157. DOI 10.1016/j.ijbiomac.2016.01.017.

Cassano, R., Trombino, S., Bloise, E., Muzzalupo, R., Iemma, F., Chidichimo, G., Picci, N., 2007. New broom fiber (spartium junceum l.) derivatives: Preparation and characterization. J. Agric. Food Chem. 55(23), 9489–9495. Available from https://www.ncbi.nlm.nih.gov/pubmed/17944531. DOI 10.1021/jf071711k.

Cassano, R., Trombino, S., Ferrarelli, T., Mezzalupo, R., Tavano, L., Picci, N., 2009. Synthesis and antibacterial activity evaluation of a novel cotton fiber (gossypium barbadense) ampicillin derivative. Carbohydr. Polym. 78 (3), 639–641.

Cassano, R., Trombino, S., Ferrarelli, T., Barone, E., Arena, V., Mancuso, C., Picci, N., 2010. Synthesis, characterization, and anti-inflammatory activity of diclofenac-bound cotton fibers. Biomacromolecules 11(7), 1716–1720. Available from https://www.ncbi.nlm.nih.gov/pubmed/20536117. DOI 10.1021/bm100404q.

Cockerham, R., Liu, S., Cachope, R., Kiyokage, E., Cheer, J.F., Shipley, M.T., Puche, A.C., 2016. Subsecond regulation of synaptically released dopamine by COMT in the olfactory bulb. J. Neurosci. 36(29), 7779–7785. Available from https://www.ncbi.nlm.nih.gov/pubmed/27445153. DOI 10.1523/JNEUROSCI.0658-16.2016.

Dash, M., Chiellini, F., Ottenbrite, R.M., Chiellini, E., 2011. Chitosan—a versatile semi-synthetic polymer in biomedical applications. Prog. Polym. Sci. 36 (8), 981–1014.

De Giglio, E., Trapani, A., Cafagna, D., Sabbatini, L., Cometa, S., 2011. Dopamine-loaded chitosan nanoparticles: Formulation and analytical characterization. Anal. Bioanal. Chem. 400(7), 1997–2002. Available from https://www.ncbi.nlm.nih.gov/pubmed/21523332. DOI 10.1007/s00216-011-4962-y.

Denora, N., Cassano, T., Laquintana, V., Lopalco, A., Trapani, A., Cimmino, C.S., Laconca, L., Giuffrida, A., Trapani, G., 2012. Novel codrugs with gabaergic activity for dopamine delivery in the brain. Int. J. Pharm. 437(1-2), 221–231. Available from https://www.ncbi.nlm.nih.gov/pubmed/22940209. DOI 10.1016/j.ijpharm.2012.08.023.

Di Gioia, M.L., Barattucci, A., Bonaccorsi, P., Leggio, A., Minuti, L., Romio, E., Temperini, A., Siciliano, C., 2014. Deprotection/reprotection of the amino group in α-amino acids and peptides. A one-pot procedure in [Bmim][BF4] ionic liquid. RCS Adv 4 (6), 2678–2686.

Di Gioia, S., Trapani, A., Mandracchia, D., De Giglio, E., Cometa, S., Mangini, V., Arnesano, F., Belgiovine, G., Castellani, S., Pace, L., Lavecchia, M.A., Trapani, G., Conese, M., Puglisi, G., Cassano, T., 2015. Intranasal delivery of dopamine to the striatum using glycol chitosan/sulfobutylether-beta-cyclodextrin based nanoparticles. Eur. J. Pharm. Biopharm. 94, 180–193. Available from http://www.ncbi.nlm.nih.gov/pubmed/26032293. DOI 10.1016/j.ejpb.2015.05.019 S0939-6411(15)00251-9 [pii].

Di Gioia, M.L., Costanzo, P., De Nino, A., Maiuolo, L., Nardi, M., Olivito, F., Procopio, A., 2017. Simple and efficient Fmoc removal in ionic liquid. RSC Adv. 7 (58), 36482–36491.

Di Stefano, A., Sozio, P., Iannitelli, A., Cerasa, L.S., 2009. New drug delivery strategies for improved parkinson's disease therapy. Expert. Opin. Drug Deliv. 6(4), 389–404. Available from https://www.ncbi.nlm.nih.gov/pubmed/19382882. DOI 10.1517/17425240902870405.

Fan, C., Fu, J., Zh,u, W., Wang, D.A., 2016. A mussel-inspired double-crosslinked tissue adhesive intended for internal medical use. Acta Biomater 33, 51–63. Available from https://www.ncbi.nlm.nih.gov/pubmed/26850148. DOI 10.1016/j.actbio.2016.02.003.

Feng, Y., He, H., Li, F., Lu, Y., Qi, J., Wu, W., 2018. An update on the role of nanovehicles in nose-to-brain drug delivery. Drug Discov. Today 23(5), 1079–1088. Available from https://www.ncbi.nlm.nih.gov/pubmed/29330120. DOI 10.1016/j.drudis.2018.01.005.

Franssen, E.H., de Bree, F.M., Verhaagen, J., 2007. Olfactory ensheathing glia: Their contribution to primary olfactory nervous system regeneration and their regenerative potential following transplantation into the injured spinal cord. Brain Res. Rev. 56(1), 236–258. Available from https://www.ncbi.nlm.nih.gov/pubmed/17884174. DOI 10.1016/j.brainresrev.2007.07.013.

Hawthorne, G.H., Bernuci, M.P., Bortolanza, M., Tumas, V., Issy, A.C., Del-Bel, E., 2016. Nanomedicine to overcome current parkinson's treatment liabilities: A systematic review. Neurotox Res. 30(4), 715–729. Available from https://www.ncbi.nlm.nih.gov/pubmed/27581037. DOI 10.1007/s12640-016-9663-z.

Ivarsson, D., Wahlgren, M., 2012. Comparison of in vitro methods of measuring mucoadhesion: Ellipsometry, tensile strength and rheological measurements. Colloids Surf. B Biointerfaces 92, 353–359. Available from https://www.ncbi.nlm.nih.gov/pubmed/22209653. DOI 10.1016/j.colsurfb.2011.12.020.

Jabli, M., Hassine, B.B., 2018. Improved removal of dyes by [sodium alginate/4-methyl-2-(naphthalen-2-yl)-N-propylpentanamide-functionalized ethoxy-silica] composite gel beads. Int. J. Biol. Macromol. 117, 247–255. Available from https://www.ncbi.nlm.nih.gov/pubmed/29807078. DOI 10.1016/j.ijbiomac.2018.04.194.

Juriga, D., Laszlo, I., Ludanyi, K., Klebovich, I., Chae, C.H., Zrinyi, M., 2018. Kinetics of dopamine release from poly(aspartamide)-based prodrugs. Acta Biomater. 76, 225–238. Available from https://www.ncbi.nlm.nih.gov/pubmed/29940369. DOI 10.1016/j.actbio.2018.06.030.

Kalčić, I., Zorc, B., Butula, I., 1996. Macromolecular prodrugs. VII. Polymer-dopamine conjugates. Int. J. Pharm. 136 (1–2), 31–36.

Kim, H.H., Park, J.B., Kang, M.J., Park, Y.H., 2014. Surface-modified silk hydrogel containing hydroxyapatite nanoparticle with hyaluronic acid-dopamine conjugate. Int. J. Biol. Macromol. 70, 516–522. Available from https://www.ncbi.nlm.nih.gov/pubmed/24999272. DOI 10.1016/j.ijbiomac.2014.06.052.

Kim, K., Kim, K., Ryu, J.H., Lee, H., 2015. Chitosan-catechol: A polymer with long-lasting mucoadhesive properties. Biomaterials 52, 161–170. Available from https://www.ncbi.nlm.nih.gov/pubmed/25818422. DOI 10.1016/j.biomaterials.2015.02.010.

Klemm, D., Philipp, B., Heinze, T., Heinze, U., Wagenknecht, W., 1998. Fundamentals and analytical methods. Wiley-VCH Verlag GmbH, Weinheim.

Kordower, J.H., Olanow, C.W., Dodiya, H.B., Chu, Y., Beach, T.G., Adler, C.H., Halliday, G.M., Bartus, R.T., 2013. Disease duration and the integrity of the nigrostriatal system in Parkinson's disease. Brain 136, 2419–2431. https://doi.org/10.1093/brain/awt192.

Kura, A.U., Al Ali, S.H.H., Hussein, M.Z., Fakurazi, S., Arulselvan, P., 2013. Development of a controlled-release anti-parkinsonian nanodelivery system using levodopa as the active agent. Int. J. Nanomed. 8, 1103–1110. Available from https://www.ncbi.nlm.nih.gov/pubmed/23524513. DOI 10.2147/IJN.S39740.

Leme Silva, A.G., Nagai, M.H., Malnic, B., 2018. Fluorescence-activated cell sorting of olfactory sensory neuron subpopulations. In: Simoes de Souza, F.M, Antunes, G.(Eds.), Olfactory receptors: Methods and protocols in molecular biology. Humana Press, New York, pp: 69–76.

Li, Y., Zhou, Y., Qi, B., Gong, T., Sun, X., Fu, Y., Zhang, Z., 2014. Brain-specific delivery of dopamine mediated by n,n-dimethyl amino group for the treatment of parkinson's disease. Mol. Pharm. 11(9), 3174–3185. Available from https://www.ncbi.nlm.nih.gov/pubmed/25072272. DOI 10.1021/mp500352p.

Liu, X., Cao, J., Li, H., Li, J., Jin, Q., Ren, K., Ji, J., 2013. Mussel-inspired polydopamine: A biocompatible and ultrastable coating for nanoparticles in vivo. ACS Nano 7(10), 9384–9395. Available from https://www.ncbi.nlm.nih.gov/pubmed/24010584. DOI 10.1021/nn404117j.

Mandracchia, D., Trapani, A., Tripodo, G., Perrone, M.G., Giammona, G., Trapani, G., Colabufo, N.A., 2017a. In vitro evaluation of glycol chitosan based formulations as oral delivery systems for efflux pump inhibition. Carbohydr. Polym. 166, 73–82. Available from https://www.ncbi.nlm.nih.gov/pubmed/28385250. DOI 10.1016/j.carbpol.2017.02.096.

Mandracchia, D., Rosato, A., Trapani, A., Chlapanidas, T., Montagner, I.M., Perteghella, S., Di Franco, C., Torre, M.L., Trapani, G., Tripodo, G., 2017b. Design, synthesis and evaluation of biotin decorated inulin based polymeric micelles as long-circulating nanocarriers for targeted drug delivery. Nanomed. Nanotechnol. Biol. Med. 13 (3), 1245–1254.

Md, S., Haque, S., Fazil, M., Kumar, M., Baboota, S., Sahni, J.K., Ali, J., 2014. Optimised nanoformulation of bromocriptine for direct nose-to-brain delivery: Biodistribution, pharmacokinetic and dopamine estimation by ultra-HPLC/mass spectrometry method. Expert. Opin Drug Deliv. 11(6), 827–842. Available from https://www.ncbi.nlm.nih.gov/pubmed/24655115. DOI 10.1517/17425247.2014.894504.

Mistry, A., Stolnik, S., Illum, L., 2009. Nanoparticles for direct nose-to-brain delivery of

drugs. Available from. Int. J. Pharm. 379 (1), 146–157. http://www.ncbi.nlm.nih.gov/entrez/query.fcgi?cmd=Retrieve&db=PubMed&dopt=Citation&list_uids=19555750.

Mistry, A., Stolnik, S., Illum, L., 2015. Nose-to-brain delivery: Investigation of the transport of nanoparticles with different surface characteristics and sizes in excised porcine olfactory epithelium. Mol. Pharm. 12(8), 2755–2766. Available from http://www.ncbi.nlm.nih.gov/pubmed/25997083. DOI 10.1021/acs.molpharmaceut.5b00088.

Musumeci, T., Pellitteri, R., Spatuzza, M., Puglisi, G., 2014. Nose-to-brain delivery: Evaluation of polymeric nanoparticles on olfactory ensheathing cells uptake. J. Pharm. Sci. 103(2), 628–635. Available from https://www.ncbi.nlm.nih.gov/pubmed/24395679. DOI 10.1002/jps.23836.

Nagatsu, T., Nakashima, A., Ichinose, H., Kobayashi, K., 2019. Human tyrosine hydroxylase in Parkinson's disease and in related disorders. J. Neural Transm. 126 (4), 397–409. https://doi.org/10.1007/s00702-018-1903-3.

Neto, A.I., Cibrao, A.C., Correia, C.R., Carvalho, R.R., Luz, G.M., Ferrer, G.G., Botelho, G., Picart, C., Alves, N.M., Mano, J.F., 2014. Nanostructured polymeric coatings based on chitosan and dopamine-modified hyaluronic acid for biomedical applications. Small, 10(12), 2459-2469. Available from https://www.ncbi.nlm.nih.gov/pubmed/24616168. DOI 10.1002/smll.201303568.

Pagar, S.A., Shinkar, D.M., Saudagar, R.B., 2014. Development and evaluation of in situ nasal mucoadhesive gel of metoprolol succinate by using 3^2 full factorial design. Int. J. Pharm. Pharm. Sci. 6 (11), 218–223.

Pahuja, R., Seth, K., Shukla, A., Shukla, R.K., Bhatnagar, P., Chauhan, L.K., Saxena, P.N., Arun, J., Chaudhari, B.P., Patel, D.K., Singh, S.P., Shukla, R., Khanna, V.K., Kumar, P., Chaturvedi, R.K., Gupta, K.C., 2015. Trans-blood brain barrier delivery of dopa- mine-loaded nanoparticles reverses functional deficits in parkinsonian rats. ACS Nano 9(5), 4850–4871. Available from https://www.ncbi.nlm.nih.gov/pubmed/25825926. DOI 10.1021/nn506408v.

Palazzo, C., Trapani, G., Ponchel, G., Trapani, A., Vauthier, C., 2017. Mucoadhesive properties of low molecular weight chitosan- or glycol chitosan- and corresponding thiomer-coated poly(isobutylcyanoacrylate) core-shell nanoparticles. Eur. J. Pharm. Biopharm. 117, 315–323. Available from https://www.ncbi.nlm.nih.gov/pubmed/28455206. DOI 10.1016/j.ejpb.2017.04.020.

Pellitteri, R., Cova, L., Zaccheo, D., Silani, V., Bossolasco, P., 2016. Phenotypic modulation and neuroprotective effects of olfactory ensheathing cells: A promising tool for cell therapy. Stem. Cell Rev. Rep. 12(2), 224–234. Available from https://www.ncbi.nlm.nih.gov/pubmed/26553037. DOI 10.1007/s12015-015-9635-3.

Pillay, S., Pillay, V., Choonara, Y.E., Naidoo, D., Khan, R.A., du Toit, L.C., Ndesendo, V. M., Modi, G., Danckwerts, M.P., Iyuk,e, S.E. 2009. Design, biometric simulation and optimization of a nano-enabled scaffold device for enhanced delivery of dopamine to the brain. Int. J. Pharm. 382(1-2), 277–290. Available from https://www.ncbi.nlm.nih.gov/pubmed/19703530. DOI 10.1016/j.ijpharm.2009.08.021.

Poinard, B., Kamaluddin, S., Tan, A.Q.Q., Neoh, K.G., Kah, J.C.Y., 2019. Polydopamine coating enhances mucopenetration and cell uptake of nanoparticles. ACS Appl. Mater. Interfaces 11(5), 4777–4789. Available from https://www.ncbi.nlm.nih.gov/pubmed/30694045. DOI 10.1021/acsami.8b18107.

Rashed, E.R., Abd El-Rehim, H.A., El-Ghazaly, M.A., 2015. Potential efficacy of dopamine loaded-PVP/PAA nanogel in experimental models of parkinsonism: Possible disease modifying activity. J. Biomed. Mater. Res. A 103(5), 1713–1720. Available from https://www.ncbi.nlm.nih.gov/pubmed/25131611. DOI 10.1002/jbm.a.35312.

Re, F., Gregori, M., Masserini, M., 2012. Nanotechnology for neurodegenerative disorders. Maturitas 73(1), 45–51. Available from https://www.ncbi.nlm.nih.gov/pubmed/22261367. DOI 10.1016/j.maturitas.2011.12.015.

Rodriguez-Nogales, C., Garbayo, E., Carmona-Abellan, M.M., Luquin, M.R., Blanco-Prieto, M.J., 2016. Brain aging and parkinson's disease: New therapeutic approaches using drug delivery systems. Maturitas 84, 25–31. Available from https://www.ncbi.nlm.nih.gov/pubmed/26653838. DOI 10.1016/j.maturitas.2015.11.009.

Rossi, S., Ferrari, F., Bonferoni, M.C., Caramella, C., 2000. Characterization of chitosan hydrochloride-mucin interaction by means of viscosimetric and turbidimetric measurements. Eur. J. Pharm. Sci. 10 (4), 251–257. https://www.ncbi.nlm.nih.gov/pubmed/10838014.

Samaridou, E., Alonso, M.J., 2018. Nose-to-brain peptide delivery - the potential of nanotechnology. Bioorg. Med. Chem. 26(10), 2888–2905. Available from https://www.ncbi.nlm.nih.gov/pubmed/29170026. DOI 10.1016/j.bmc.2017.11.001.

Saraiva, C., Praca, C., Ferreira, R., Santos, T., Ferreira, L., Bernardino, L., 2016. Nanoparticle-mediated brain drug delivery: Overcoming blood-brain barrier to treat neurodegenerative diseases. J. Control Release 235, 34–47. Available from https://www.ncbi.nlm.nih.gov/pubmed/27208862. DOI 10.1016/j.jconrel.2016.05.044.

Shi, Y., Xu, D., Liu, M., Fu, L., Wan, Q., Mao, L., Dai, Y., Wen, Y., Zhang, X., Wei, Y., 2018. Room temperature preparation of fluorescent starch nanoparticles from starch-dopamine conjugates and their biological applications. Mater. Sci. Eng. C Mater. Biol. Appl. 82, 204–209. Available from https://www.ncbi.nlm.nih.gov/pubmed/29025649. DOI 10.1016/j.msec.2017.08.070.

Smistad, G., Nyström, B., Zhu, K., Grønvold, M.K., Røv-Johnsen, A., Hiorth, M., 2017. Liposomes coated with hydrophobically modified hydroxyethyl cellulose: Influence of hydrophobic chain length and degree of modification. Colloids Surf. B Biointerfaces 156, 79–86. https://doi.org/10.1016/j.colsurfb.2017.04.061.

Sogias, I.A., Williams, A.C., Khutoryanskiy, V.V., 2008. Why is chitosan mucoadhesive? Biomacromolecules 9(7), 837–1842. Available from https://www.ncbi.nlm.nih.gov/pubmed/18540644. DOI 10.1021/bm800276d.

Tan, M.E., He, C.H., Jiang, W., Zeng, C., Yu, N., Huang, W., Gao, Z.G., Xing, J.G., 2017. Development of solid lipid nanoparticles containing total flavonoid extract from dracocephalum moldavica L. and their therapeutic effect against myocardial ischemia-reperfusion injury in rats. Int. J. Nanomed. 12, 3253–3265. Available from https://www.ncbi.nlm.nih.gov/pubmed/28458544. DOI 10.2147/IJN.S131893.

Trapani, A., De Giglio, E., Cafagna, D., Denora, N., Agrimi, G., Cassano, T., Gaetani, S., Cuomo, V., Trapani, G., 2011. Characterization and evaluation of chitosan nanoparticles for dopamine brain delivery. Int. J. Pharm. 419 (1–2), 296–307. http://www.ncbi.nlm.nih.gov/entrez/query.fcgicmd=Retrieve&db=PubMed&dopt=Citation&list_uid.

Trapani, A., Palazzo, C., Contino, M., Perrone, M.G., Cioffi, N., Ditaranto, N., Colabufo, N. A., Conese, M., Trapani, G., Puglisi, G., 2014. Mucoadhesive properties and interaction with P-glycoprotein (P-gp) of thiolated-chitosans and -glycol chitosans and corresponding parent polymers: A comparative study. Biomacromolecules 15(3), 882–893. Available from http://www.ncbi.nlm.nih.gov/pubmed/24521085. DOI 10.1021/bm401733p.

Trapani, A., Tricarico, D., Mele, A., Maqoud, F., Mandracchia, D., Vitale, P., Capriati, V., Trapani, G., Dimiccoli, V., Tolomeo, A., Scilimati, A., 2017. A novel injectable formulation of 6-fluoro-L-DOPA imaging agent for diagnosis of neuroendocrine tumors and parkinson's disease. Int. J. Pharm. 519 (1–2), 304–313. https://doi.org/10.1016/j.ijpharm.2017.01.038.

Trapani, A., Mandracchia, D., Tripodo, G., Cometa, S., Cellamare, S., De Giglio, E., Klepetsanis, P., Antimisiaris, S.G., 2018. Protection of dopamine towards autoxidation reaction by encapsulation into non-coated- or chitosan- or thiolated chitosan-coated-liposomes. Colloids Surf. B Biointerfaces 170, 11-19. Available from https://www.ncbi.nlm.nih.gov/pubmed/29859476. DOI 10.1016/j.colsurfb.2018.05.049.

Walker, R.B., Ayres, J.W., Block, J.H., Lock, A., 1978. Tert-butoxycarbanyl as a convenient protecting group in synthesis of potential centrally active dopamine derivatives. J. Pharm. Sci. 67(4), 558–559. Available from https://www.ncbi.nlm.nih.gov/pubmed/641771. DOI 10.1002/jps.2600670433.

Yang, H., He, B.R., Hao, D.J., 2015. Biological roles of olfactory ensheathing cells in facilitating neural regeneration: A systematic review. Mol. Neurobiol. 51(1), 168–179. Available from https://www.ncbi.nlm.nih.gov/pubmed/24615159. DOI 10.1007/s12035-014-8664-2.